

Computer-Oriented Representations of *RS*-Stereoisomeric Groups and Cycle Indices with Chirality Fittingness (CI-CFs) Calculated by the GAP System. Enumeration of *RS*-Stereoisomers by Fujita's Proligand Method

Shinsaku Fujita

*Shonan Institute of Chemoinformatics and Mathematical Chemistry,
Kaneko 479-7 Ooimachi, Ashigara-Kami-Gun, Kanagawa-Ken,
258-0019 Japan*

shinsaku.fujita@nifty.com

(Received June 15, 2016)

Abstract

A point group for specifying chirality and an *RS*-permutation group for specifying *RS*-stereogenicity are differentiated by means of mirror-coset representations. They are integrated to generate an *RS*-stereoisomeric group, after the computer-oriented representation of the *RS*-stereoisomeric group has been developed by starting from mirror-coset representations. Thereby, the processes of combinatorial enumeration are computerized on the basis of the GAP system. The construction of an *RS*-stereoisomeric group stems from an appropriate generators by using the `Group` function of the GAP system. The calculation of the corresponding cycle index with chirality fittingness (CI-CF) is based on the function `CalcConjClassCICF` developed as a function of the GAP system. The calculation of the corresponding generating function and the evaluation of the coefficient of each term are conducted by using newly-developed GAP functions. The source lists of practical procedures for combinatorial enumeration of 3D structures are attached as appendices.

1 Introduction

From the beginning of stereochemistry, chirality has been presumed to be a single kind of handedness for supporting both van't Hoff's way [1,2] and Le Bel's way [3,4], even though the former depends on "asymmetry" [1, 2] (or later, stereogenicity [5]) and the latter depends on "dissymmetry" [6] (or later, chirality [7]). In particular, even van't Hoff's way (asymmetry, stereogenicity) has been linked to chirality as the single kind of handedness, because modern stereochemistry has not recognized handedness other than chirality. This misleadingly linkage without recognizing another kind of handedness has provided serious confusion to the terminology of modern stereochemistry, e.g.. "pseudoasymmetry" as an exception of "asymmetry" [8–10] and "chirality units" as a subcategory of "stereogenic units" [11, 12]. Although there appeared several discussions on the serious confusion [13–16] and several revisions of terminology [11, 12, 17], they have not yet recognized handedness other than chirality, so that they have revealed their limitations because of unconscious transmutation of terminology, as pointed out in my review [18].

To settle the confusion in the terminology of modern stereochemistry, the stereoisogram approach has been proposed by the author (Fujita) [19–21]. One of the most important conclusions of Fujita's stereoisogram approach is that there are two kinds of handedness, i.e., chirality and *RS*-stereogenicity, where the concept of *RS*-stereogenicity has been proposed as a substantial restriction of "stereogenicity" in order to demonstrate the net interaction between chirality and (unrestricted) stereogenicity. The two kinds of handedness (chirality and *RS*-stereogenicity) are integrated to generate *RS*-stereoisomerism, which is characterized by *RS*-stereoisomeric groups as algebraic expressions and by stereoisograms as diagrammatic expressions. Thereby, the theoretical foundations of modern stereochemistry have been restructured to give a self-consistent framework [22–25]. Fujita's stereoisogram approach has effectively remedied discontents of stereochemical terminology [18].

A quadruplet of *RS*-stereoisomers contained in a stereoisogram is an equivalence class under the action of an *RS*-stereoisomeric group. This means that inequivalent quadruplets can be enumerated combinatorially under an *RS*-stereoisomeric group. After unit subduced cycle indices with chirality fittingness (USCI-CFs) of Fujita's USCI approach [26–28] have been extended to meet *RS*-stereoisomeric groups, symmetry-itemized enumeration of quadruplets of *RS*-stereoisomers have been conducted to count tetrahedral

derivatives [29, 30], allene derivatives [31, 32], and oxirane derivatives [33].

Type-itemized enumeration of quadruplets of *RS*-stereoisomers has been conducted under the action of *RS*-stereoisomeric groups [34], where cycles indices of chirality fittingness (CI-CFs) proposed originally in Fujita's proligand method [35–38] have been extended to meet the requirement of *RS*-stereoisomeric groups. More systematic methods for type-itemized enumeration have been developed by proposing modulated CI-CFs [39–41].

From the computational viewpoint of enumeration practice, there are two phases to be considered during the above-mentioned enumerations, i.e., calculation of USCI-CFs (for Fujita's USCI approach) or CI-CFs (for Fujita's proligand method) and calculation of generating functions. Although the latter phase has been effectively conducted by using computer, the calculation of USCI-CFs or CI-CFs has not yet computerized especially in the extended usage for *RS*-stereoisomeric groups. This is because there have been no effective (computer-oriented) representations for differentiating between two subgroups of *RS*-stereoisomeric groups, i.e., point groups and *RS*-permutation groups.

I have recently proposed the computer-oriented representations of point groups, where GAP functions for calculating CI-CFs have been developed [42, 43]. The next task is to develop the computer-oriented representations of *RS*-stereoisomeric groups, which are capable of differentiating between point subgroups and *RS*-permutation subgroups. Thereby, the calculation of CI-CFs as well as the calculation of generating functions will be computerized in the extended usage for *RS*-stereoisomeric groups.

2 Combined Representations of *RS*-Stereoisomeric Groups

2.1 *RS*-Stereoisomeric Groups and Stereoisograms

According to Fujita's stereoisogram approach [19–21], chirality under point-group symmetry (the first kind of handedness) and *RS*-stereogenicity under *RS*-permutation-group symmetry (the second kind of handedness) are integrated to give *RS*-stereoisomerism as a new concept, where the two groups are combined with a ligand-reflection group as an additional group, so as to develop an *RS*-stereoisomeric group. Such an *RS*-stereoisomeric group is illustrated by a stereoisogram, which is developed as a diagrammatic expression as shown by Figure 1.

The vertical direction of a stereoisogram (e.g., Figure 1) is concerned with chirali-

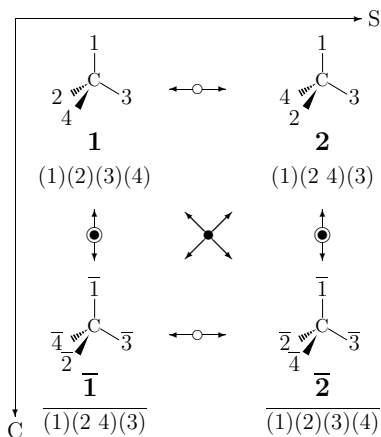


Figure 1. Elementary stereoisogram of numbered tetrahedral skeletons. The other modes of sequential numbering are permitted without losing generality.

ty/achirality under point-group symmetry (e.g., \mathbf{T}_d). A reflection (e.g., $\overline{(1)(2\ 4)(3)}$) converts a numbered skeleton (e.g., **1**) into the corresponding mirror-numbered skeleton (e.g., $\overline{\mathbf{1}}$). The original numbered skeleton (e.g., **1**) and the mirror-numbered skeleton (e.g., $\overline{\mathbf{1}}$) are enantiomeric to each other, where the reflection (e.g., $\overline{(1)(2\ 4)(3)}$) is accompanied by a ligand reflection, which is emphasized by attaching an overline.

The horizontal direction of a stereoisogram (e.g., Figure 1) is concerned with *RS*-stereogenicity/*RS*-astereogenicity under *RS*-permutation-group symmetry (e.g., \mathbf{T}_8). An *RS*-permutation (e.g., $(1)(2\ 4)(3)$) converts the numbered skeleton (e.g., **1**) into the corresponding *RS*-numbered skeleton (e.g., **2**). The original numbered skeleton (e.g., **1**) and the *RS*-numbered skeleton (e.g., **2**) are *RS*-diastereomeric to each other, where the *RS*-permutation (e.g., $(1)(2\ 4)(3)$) is not accompanied by a ligand reflection.

The diagonal direction of a stereoisogram (e.g., Figure 1) is concerned with sclerality/asclerality under ligand-reflection-group symmetry (e.g., \mathbf{T}_7). A ligand reflection (e.g., $\overline{(1)(2)(3)(4)}$) converts the numbered skeleton (e.g., **1**) into the corresponding LR-numbered skeleton (e.g., $\overline{\mathbf{2}}$). The original numbered skeleton (e.g., **1**) and the LR-numbered skeleton (e.g., $\overline{\mathbf{2}}$) are holantimeric to each other, where the ligand reflection (e.g., $\overline{(1)(2)(3)(4)}$) is accompanied by a ligand reflection, which is emphasized by attaching an overline.

A quadruplet of numbered skeletons contained in a stereoisogram (e.g., Figure 1) is controlled by an *RS*-stereoisomeric group (e.g., $\mathbf{T}_{d\bar{\sigma}\bar{\tau}}$), which is generated by integrating the three groups, i.e., a point group (e.g., \mathbf{T}_d), an *RS*-permutation group (e.g., $\mathbf{T}_{\bar{\sigma}}$), and a ligand-reflection group (e.g., $\mathbf{T}_{\bar{\tau}}$).

For further investigation of Fujita's stereoisogram approach, expressions using an overline (e.g., $\overline{(1)(2)(3)(4)}$ and $\overline{(1)(2)(3)(4)}$) should be replaced by computer-oriented representations, which enable us to treat ligand reflections more systematically by computer.

2.2 Combined Representations of Point Groups

Let us consider a set of n positions of a given skeleton:

$$\mathbf{X} = \{1, 2, 3, \dots, n\}, \quad (1)$$

where the positions are numbered sequentially. The set can be regarded as belonging to different groups according to viewpoints of our discussions.

The action of a point group $\overline{\mathbf{G}}$ on \mathbf{X} (Eq. 1) brings about a permutation representation $\mathbf{P}_{\overline{\mathbf{G}}}^{(\mathbf{X})}$, where the effect of ligand reflections is not taken into consideration. The point group $\overline{\mathbf{G}}$ has a maximum chiral subgroup $\mathbf{G}^{(m)}$, so that the following coset decomposition is obtained:

$$\overline{\mathbf{G}} = \mathbf{G}^{(m)} + \mathbf{G}^{(m)}\sigma, \quad (2)$$

where the symbol σ represents a (roto)reflection selected appropriately. To evaluate the effect of ligand reflections, a two-membered set of cosets is taken into consideration:

$$\overline{\chi} = \{\mathbf{G}^{(m)}, \mathbf{G}^{(m)}\sigma\}. \quad (3)$$

The action of the point group $\overline{\mathbf{G}}$ on the set $\overline{\chi}$ produces a coset representation of degree 2 (called a *mirror-coset representation*):

$$\mathbf{P}_{\overline{\mathbf{G}}}^{(\overline{\chi})} = \{\mathbf{P}_g^{(\overline{\chi})} \mid \forall g \in \overline{\mathbf{G}}\}, \quad (4)$$

Table 1. *RS*-Stereoisomeric Group $T_{d\hat{\sigma}\hat{\tau}}$ and its Subgroups for Characterizing a Tetrahedral Skeleton

group	a list of generators, order, a list of elements
T_d (point group)	<pre>Td := Group([(1,3)(2,4), (2,3,4), (1,3)(5,6)]) Order = 24 [(), (3,4)(5,6), (2,3)(5,6), (2,3,4), (2,4,3), (2,4)(5,6), (1,2)(5,6), (1,2)(3,4), (1,2,3), (1,2,3,4)(5,6), (1,2,4,3)(5,6), (1,2,4), (1,3,2), (1,3,4,2)(5,6), (1,3)(5,6), (1,3,4), (1,3)(2,4), (1,3,2,4)(5,6), (1,4,3,2)(5,6), (1,4,2), (1,4,3), (1,4)(5,6), (1,4,2,3)(5,6), (1,4)(2,3)]</pre>
$T_{\hat{\sigma}}$ (<i>RS</i> -permutation group)	<pre>Ts := Group([(1,3)(2,4), (2,3,4), (1,3)]) Order = 24 [(), (3,4), (2,3), (2,3,4), (2,4,3), (2,4), (1,2), (1,2)(3,4), (1,2,3), (1,2,3,4), (1,2,4,3), (1,2,4), (1,3,2), (1,3,4,2), (1,3), (1,3,4), (1,3)(2,4), (1,3,2,4), (1,4,3,2), (1,4,2), (1,4,3), (1,4), (1,4,2,3), (1,4)(2,3)]</pre>
$T_{\hat{\tau}}$ (ligand-reflection group)	<pre>TI := Group([(1,3)(2,4), (2,3,4), (5,6)]) Order = 24 [(), (5,6), (2,3,4), (2,3,4)(5,6), (2,4,3), (2,4,3)(5,6), (1,2)(3,4), (1,2)(3,4)(5,6), (1,2,3), (1,2,3)(5,6), (1,2,4), (1,2,4)(5,6), (1,3,2), (1,3,2)(5,6), (1,3,4), (1,3,4)(5,6), (1,3)(2,4), (1,3)(2,4)(5,6), (1,4,2), (1,4,2)(5,6), (1,4,3), (1,4,3)(5,6), (1,4)(2,3), (1,4)(2,3)(5,6)]</pre>
T (normal subgroup)	<pre>T := Group([(1,3)(2,4), (2,3,4)]) Order = 12 [(), (2,3,4), (2,4,3), (1,2)(3,4), (1,2,3), (1,2,4), (1,3,2), (1,3,4), (1,3)(2,4), (1,4,2), (1,4,3), (1,4)(2,3)]</pre>
$T_{d\hat{\sigma}\hat{\tau}}$ (<i>RS</i> -stereoisomeric group)	<pre>TdsI := Group([(1,3)(2,4), (2,3,4), (1,3)(5,6), (5,6)]) Order = 48 [(), (5,6), (3,4), (3,4)(5,6), (2,3), (2,3)(5,6), (2,3,4), (2,3,4)(5,6), (2,4,3), (2,4,3)(5,6), (2,4), (2,4)(5,6), (1,2), (1,2)(5,6), (1,2)(3,4), (1,2)(3,4)(5,6), (1,2,3), (1,2,3)(5,6), (1,2,3,4), (1,2,3,4)(5,6), (1,2,4,3), (1,2,4,3)(5,6), (1,2,4), (1,2,4)(5,6), (1,3,2), (1,3,2)(5,6), (1,3,4,2), (1,3,4,2)(5,6), (1,3), (1,3)(5,6), (1,3,4), (1,3,4)(5,6), (1,3)(2,4), (1,3)(2,4)(5,6), (1,3,2,4), (1,3,2,4)(5,6), (1,4,3,2), (1,4,3,2)(5,6), (1,4,2), (1,4,2)(5,6), (1,4,3), (1,4,3)(5,6), (1,4), (1,4)(5,6), (1,4,2,3), (1,4,2,3)(5,6), (1,4)(2,3), (1,4)(2,3)(5,6)]</pre>

each permutation of which is represented as follows:

$$\begin{aligned} \mathbf{P}_g^{(\bar{x})} &= \begin{pmatrix} \mathbf{G}^{(m)} & \mathbf{G}^{(m)}\sigma \\ \mathbf{G}^{(m)} & \mathbf{G}^{(m)}\sigma \end{pmatrix} \\ &= \begin{pmatrix} n+1 & n+2 \\ n+1 & n+2 \end{pmatrix} = (n+1)(n+2) \quad \text{for } \forall g \in \mathbf{G}^{(m)}: \text{ rotations} \end{aligned} \quad (5)$$

$$\begin{aligned} \mathbf{P}_g^{(\bar{x})} &= \begin{pmatrix} \mathbf{G}^{(m)} & \mathbf{G}^{(m)}\sigma \\ \mathbf{G}^{(m)}\sigma & \mathbf{G}^{(m)} \end{pmatrix} \\ &= \begin{pmatrix} n+1 & n+2 \\ n+2 & n+1 \end{pmatrix} = (n+1 \ n+2) \quad \text{for } \forall g \in \mathbf{G}^{(m)}\sigma: \text{ (roto)reflections} \end{aligned} \quad (6)$$

Although the mirror-coset representation $\mathbf{P}_{\bar{e}}^{(\bar{x})}$ (Eq. 4) is based on the set of cosets (Eq. 3), it brings about an equivalent effect to a mirror-permutation representation (Eq. 6 of [42]), which has been previously defined on the basis of the set of local chiralities (Eq. 3 of [42]).

Because the permutation representation $\mathbf{P}_{\bar{e}}^{(\mathbf{x})}$ described above is concerned with the n positions of \mathbf{X} (Eq. 1), the subsequent numbering $n+1$ and $n+2$ is adopted in Eqs. 5 and 6. The permutation representation $\mathbf{P}_{\bar{e}}^{(\mathbf{x})}$ is combined with the permutation representation $\mathbf{P}_{\bar{e}}^{(\bar{x})}$ (Eq. 4) to give a *combined-permutation representation*:

$$\mathbf{P}_{\bar{e}}^{(\mathbf{x}\bar{x})} = \mathbf{P}_{\bar{e}}^{(\mathbf{x})} \oplus \mathbf{P}_{\bar{e}}^{(\bar{x})} = \{\mathbf{P}_g^{(\mathbf{x})} \oplus \mathbf{P}_g^{(\bar{x})} \mid \forall g \in \bar{\mathbf{G}}\}, \quad (7)$$

where the symbol $\mathbf{P}_g^{(\mathbf{x})} \oplus \mathbf{P}_g^{(\bar{x})}$ is a combination of the two permutations for g at issue. The degree of the combined representation (Eq. 7) is equal to $n+2$. The combined representation (Eq. 7) based on the mirror-coset representation (Eq. 4) is equivalent to the combined representation (Eq. 7 of [42]) defined previously on the basis of the mirror-permutation representation (Eq. 6 of [42]).

The combined representation (Eq. 7) can be regarded as a permutation group isomorphic (or generally homomorphic) to the original point group $\bar{\mathbf{G}}$. For example, the point group \mathbf{T}_d for characterizing a tetrahedral skeleton $\mathbf{1}$ (the vertical direction of Figure 1) can be constructed by using the `Group` function of the GAP system, where a set of generators `gen_Td` is composed of $(1,3)(2,4)$ for a two-fold rotation, $(2,3,4)$ for a three-fold rotation, and $(1,3)(5,6)$ for a reflection with a ligand-reflection permutation $(5,6)$. Each command of the GAP system is input after a prompt `gap>` in the command prompt display of the Windows OS as follows:

```
gap> gen_Td := [(1,3)(2,4), (2,3,4), (1,3)(5,6)];;
gap> Td := Group(gen_Td);;
gap> Print("Td:=", Td, "\n");;
```

```
Td := Group( [ (1,3)(2,4), (2,3,4), (1,3)(5,6) ] )
gap> Print("Order=", Size(Td), "\n");
Order = 24
gap> element_Td := Elements(Td);
gap> Print(element_Td, "\n");
[ (), (3,4)(5,6), (2,3)(5,6), (2,3,4), (2,4,3), (2,4)(5,6), (1,2)(5,6), (1,2)(3,4), (1,2,3), (1,2,3,4)(5,6),
  (1,2,4,3)(5,6), (1,2,4), (1,3,2), (1,3,4,2)(5,6), (1,3)(5,6), (1,3,4), (1,3)(2,4), (1,3,2,4)(5,6),
  ↪ (1,4,3,2)(5,6),
  (1,4,2), (1,4,3), (1,4)(5,6), (1,4,2,3)(5,6), (1,4)(2,3) ]
```

This result is collected in the first part of Table 1. The resulting group Td (order 24) contains 24 elements, which are produced as a set of permutations (products of cycles), as listed in the list `element_Td`. These permutations are group elements corresponding to a combined representation shown generally by Eq. 7. Each (roto)reflection with an overline is represented by a permutation with (5,6). For example, the reflection $\overline{(1)(2\ 4)(3)}$ (with an overline) in Figure 1 is denoted as (2,4)(5,6) in the list `element_Td`.

2.3 Combined Representations of *RS*-Permutation Groups

The corresponding *RS*-permutation group $\tilde{\mathbf{G}}$ is generated by starting from the point group $\overline{\mathbf{G}}$, where the *RS*-permutations of $\tilde{\mathbf{G}}$ correspond to the (roto)reflections but have no effects of ligand reflections. The action of $\tilde{\mathbf{G}}$ on \mathbf{X} (Eq. 1) brings about a permutation representation $\mathbf{P}_{\tilde{\mathbf{G}}}^{(\mathbf{X})}$, where the effect of ligand reflections is not taken into consideration (i.e., degree n). Without considering the effect of ligand reflections, the permutation representation $\mathbf{P}_{\tilde{\mathbf{G}}}^{(\mathbf{X})}$ for the *RS*-permutation group $\tilde{\mathbf{G}}$ is equal to the above-mentioned permutation representation $\mathbf{P}_{\tilde{\mathbf{G}}}^{(\mathbf{X})}$ for the point group $\overline{\mathbf{G}}$ (cf. Eq. 7). The point group $\tilde{\mathbf{G}}$ contains the maximum chiral subgroup $\mathbf{G}^{(m)}$, so that the following coset decomposition is obtained:

$$\tilde{\mathbf{G}} = \mathbf{G}^{(m)} + \mathbf{G}^{(m)}\tilde{\sigma}, \quad (8)$$

where the symbol $\tilde{\sigma}$ represents an *RS*-permutation selected appropriately. To evaluate the effect of *RS*-permutations, a two-membered set of cosets is taken into consideration:

$$\tilde{\chi} = \{ \mathbf{G}^{(m)}, \mathbf{G}^{(m)}\tilde{\sigma} \}. \quad (9)$$

The action of the point group $\tilde{\mathbf{G}}$ on the set $\tilde{\chi}$ produces no effect:

$$\mathbf{P}_{\tilde{\mathbf{G}}}^{(\tilde{\chi})} = \{ \mathbf{P}_g^{(\tilde{\chi})} \mid \forall g \in \tilde{\mathbf{G}} \}, \quad (10)$$

each permutation of which is a product of two 1-cycles represented as follows:

$$\begin{aligned} \mathbf{P}_g^{(\tilde{x})} &= \begin{pmatrix} \mathbf{G}^{(m)} & \mathbf{G}^{(m)}\tilde{\sigma} \\ \mathbf{G}^{(m)} & \mathbf{G}^{(m)}\tilde{\sigma} \end{pmatrix} \\ &= \begin{pmatrix} n+1 & n+2 \\ n+1 & n+2 \end{pmatrix} = (n+1)(n+2) \quad \text{for } \forall g \in \tilde{\mathbf{G}} \end{aligned} \quad (11)$$

Because the permutation representation $\mathbf{P}_{\tilde{\mathbf{G}}}^{(\mathbf{x})}$ described above is concerned with the n positions of \mathbf{X} (Eq. 1), the subsequent numbering $n+1$ and $n+2$ is adopted in Eq. 11. The permutation representation $\mathbf{P}_{\tilde{\mathbf{G}}}^{(\mathbf{x})}$ is combined with the permutation representation $\mathbf{P}_{\tilde{\mathbf{G}}}^{(\tilde{x})}$ (Eq. 11) to give a *combined-permutation representation*:

$$\mathbf{P}_{\tilde{\mathbf{G}}}^{(\mathbf{x}\tilde{x})} = \mathbf{P}_{\tilde{\mathbf{G}}}^{(\mathbf{x})} \oplus \mathbf{P}_{\tilde{\mathbf{G}}}^{(\tilde{x})} = \{\mathbf{P}_g^{(\mathbf{x})} \oplus \mathbf{P}_g^{(\tilde{x})} \mid \forall g \in \tilde{\mathbf{G}}\}, \quad (12)$$

where the symbol $\mathbf{P}_g^{(\mathbf{x})} \oplus \mathbf{P}_g^{(\tilde{x})}$ is a combination of the two permutations for g at issue. The degree of the combined representation (Eq. 12) is equal to $n+2$.

The combined representation (Eq. 12) can be regarded as a permutation group isomorphic (or generally homomorphic) to the original point group $\tilde{\mathbf{G}}$. For example, the *RS*-permutation group $\mathbf{T}_{\tilde{\sigma}}$ for characterizing the horizontal direction of Figure 1 can be constructed by using the **Group** function of the GAP system, where a set of generators (the argument of the function **Group**) is composed of (1,3)(2,4) for a two-fold rotation, (2,3,4) for a three-fold rotation, and (1,3) for an *RS*-permutation (by omitting a ligand-reflection part (5)(6)). The commands of the GAP system and their results are shown in the $\mathbf{T}_{\tilde{\sigma}}$ -part (the second part) of Table 1. It should be noted that $\mathbf{P}_{\tilde{\mathbf{G}}}^{(\mathbf{x}\tilde{x})}$ of degree $n+2$ (e.g., $\mathbf{P}_{\tilde{\mathbf{G}}}^{(\mathbf{x}\tilde{x})}$ of degree 6) and $\mathbf{P}_{\tilde{\mathbf{G}}}^{(\mathbf{x})}$ of degree n (e.g., $\mathbf{P}_{\tilde{\mathbf{G}}}^{(\mathbf{x})}$ of degree 4) in Eq. 12 are conceptually different from each other, although their explicit expressions due to the GAP system are equal to each other.

2.4 Combined Representations of Ligand-Reflection Groups

The action of a ligand-reflection group $\hat{\mathbf{G}}$ on \mathbf{X} (Eq. 1) brings about a permutation representation $\mathbf{P}_{\hat{\mathbf{G}}}^{(\mathbf{x})}$, where the effect of ligand reflections is not taken into consideration. The ligand-reflection group $\hat{\mathbf{G}}$ contains the maximum chiral subgroup $\mathbf{G}^{(m)}$, so that the following coset decomposition is obtained:

$$\hat{\mathbf{G}} = \mathbf{G}^{(m)} + \mathbf{G}^{(m)}\hat{I}, \quad (13)$$

where the symbol \hat{I} represents a ligand reflection corresponding to the identity element I .

To evaluate the effect of ligand reflections, a two-membered set of cosets is taken into consideration:

$$\widehat{\chi} = \{ \mathbf{G}^{(m)}, \mathbf{G}^{(m)}\widehat{I} \}. \quad (14)$$

The action of the ligand-reflection group $\widehat{\mathbf{G}}$ on the set $\widehat{\chi}$ produces a coset representation of degree 2:

$$\mathbf{P}_{\widehat{\mathbf{G}}}^{(\widehat{\chi})} = \{ \mathbf{P}_g^{(\widehat{\chi})} \mid \forall g \in \widehat{\mathbf{G}} \}, \quad (15)$$

each permutation of which is represented as follows:

$$\begin{aligned} \mathbf{P}_g^{(\widehat{\chi})} &= \begin{pmatrix} \mathbf{G}^{(m)} & \mathbf{G}^{(m)}\widehat{I} \\ \mathbf{G}^{(m)} & \mathbf{G}^{(m)}\widehat{I} \end{pmatrix} \\ &= \begin{pmatrix} n+1 & n+2 \\ n+1 & n+2 \end{pmatrix} = (n+1)(n+2) \quad \text{for } \forall g \in \mathbf{G}^{(m)}: \text{ rotations} \end{aligned} \quad (16)$$

$$\begin{aligned} \mathbf{P}_g^{(\widehat{\chi})} &= \begin{pmatrix} \mathbf{G}^{(m)} & \mathbf{G}^{(m)}\widehat{I} \\ \mathbf{G}^{(m)}\widehat{I} & \mathbf{G}^{(m)} \end{pmatrix} \\ &= \begin{pmatrix} n+1 & n+2 \\ n+2 & n+1 \end{pmatrix} = (n+1 \ n+2) \quad \text{for } \forall g \in \mathbf{G}^{(m)}\widehat{I}: \text{ ligand reflections} \end{aligned} \quad (17)$$

Because the permutation representation $\mathbf{P}_{\widehat{\mathbf{G}}}^{(\mathbf{X})}$ described above is concerned with the n positions of \mathbf{X} (Eq. 1), the subsequent numbering $n+1$ and $n+2$ is adopted in Eqs. 16 and 17. The permutation representation $\mathbf{P}_{\widehat{\mathbf{G}}}^{(\mathbf{X})}$ is combined with the permutation representation $\mathbf{P}_{\widehat{\mathbf{G}}}^{(\widehat{\chi})}$ to give a *combined-permutation representation*:

$$\mathbf{P}_{\widehat{\mathbf{G}}}^{(\mathbf{X}\widehat{\chi})} = \mathbf{P}_{\widehat{\mathbf{G}}}^{(\mathbf{X})} \oplus \mathbf{P}_{\widehat{\mathbf{G}}}^{(\widehat{\chi})} = \{ \mathbf{P}_g^{(\mathbf{X})} \oplus \mathbf{P}_g^{(\widehat{\chi})} \mid \forall g \in \widehat{\mathbf{G}} \}, \quad (18)$$

where the symbol $\mathbf{P}_g^{(\mathbf{X})} \oplus \mathbf{P}_g^{(\widehat{\chi})}$ is a combination of the two permutations for g at issue. The degree of the combined representation (Eq. 18) is equal to $n+2$.

The combined representation (Eq. 18) can be regarded as a permutation group isomorphic (or generally homomorphic) to the original ligand-reflection group $\widehat{\mathbf{G}}$. For example, the ligand-reflection group $\mathbf{T}_{\widehat{\mathcal{F}}}$ for characterizing the diagonal direction of Figure 1 can be constructed by using the **Group** function of the GAP system, where a set of generators (the argument of the function **Group**) is composed of (1,3)(2,4) for a two-fold rotation, (2,3,4) for a three-fold rotation, and (5,6) for a ligand reflection. The commands of the GAP system and their results are shown in the $\mathbf{T}_{\widehat{\mathcal{F}}}$ -part (the third part) of Table 1.

This construction of the ligand-reflection group $\mathbf{T}_{\widehat{\mathcal{F}}}$ (TI) is based on the addition of the ligand reflection (5,6) to the maximum point group \mathbf{T} (T), which is in turn generated

by a set of generators $[(1,3)(2,4), (2,3,4)]$ as shown in the **T**-part (the fourth part) of Table 1.

2.5 Combined Representations of *RS*-Stereoisomeric Groups

Because the point group $\overline{\mathbf{G}}$ (Eq. 2), the *RS*-permutation group $\widetilde{\mathbf{G}}$ (Eq. 8), and the ligand-reflection group $\widehat{\mathbf{G}}$ (Eq. 13) have the maximum chiral subgroup $\mathbf{G}^{(m)}$ commonly, they are integrated to give an *RS*-stereoisomeric group \mathbf{G} as follows:

$$\mathbf{G} = \mathbf{G}^{(m)} + \mathbf{G}^{(m)}\sigma + \mathbf{G}^{(m)}\tilde{\sigma} + \mathbf{G}^{(m)}\widehat{I}. \quad (19)$$

The resulting group \mathbf{G} (Eq. 19) acts on the set \mathbf{X} (Eq. 1) to give a permutation representation $\mathbf{P}_{\mathbf{G}}^{(\mathbf{X})}$, where the effect of ligand reflections is not taken into consideration.

To evaluate the effect of ligand reflections, Eq. 19 is rewritten by referring to Eq. 8 as follows:

$$\mathbf{G} = (\mathbf{G}^{(m)} + \mathbf{G}^{(m)}\tilde{\sigma}) + (\mathbf{G}^{(m)}\sigma + \mathbf{G}^{(m)}\widehat{I}) = \widetilde{\mathbf{G}} + \widetilde{\mathbf{G}}\sigma, \quad (20)$$

where we use $\tilde{\sigma}\sigma = \widehat{I}$. Then, we take account of the following set of two cosets:

$$\chi = \{\widetilde{\mathbf{G}}, \widetilde{\mathbf{G}}\sigma\}. \quad (21)$$

The action of the *RS*-stereoisomeric group \mathbf{G} on the set χ produces a coset representation of degree 2 (also called a *mirror-coset representation*):

$$\mathbf{P}_{\mathbf{G}}^{(\chi)} = \{\mathbf{P}_g^{(\chi)} \mid \forall g \in \mathbf{G}\}, \quad (22)$$

each permutation of which is represented as follows:

$$\begin{aligned} \mathbf{P}_g^{(\chi)} &= \begin{pmatrix} \widetilde{\mathbf{G}} & \widetilde{\mathbf{G}}\sigma \\ \widetilde{\mathbf{G}} & \widetilde{\mathbf{G}}\sigma \end{pmatrix} \\ &= \begin{pmatrix} n+1 & n+2 \\ n+1 & n+2 \end{pmatrix} = (n+1)(n+2) \quad \text{for } \forall g \in \widetilde{\mathbf{G}} \end{aligned} \quad (23)$$

$$\begin{aligned} \mathbf{P}_g^{(\chi)} &= \begin{pmatrix} \widetilde{\mathbf{G}} & \widetilde{\mathbf{G}}\sigma \\ \widetilde{\mathbf{G}}\sigma & \widetilde{\mathbf{G}} \end{pmatrix} \\ &= \begin{pmatrix} n+1 & n+2 \\ n+2 & n+1 \end{pmatrix} = (n+1)(n+2) \quad \text{for } \forall g \in \widetilde{\mathbf{G}}\sigma \end{aligned} \quad (24)$$

It should be noted that Eq. 22 is consistent with Eqs. 4, 10, and 15.

The permutation representation $\mathbf{P}_{\mathbf{G}}^{(\mathbf{x})}$ is combined with the permutation representation $\mathbf{P}_{\mathbf{G}}^{(\mathbf{x})}$ (Eq. 22) to give a *combined-permutation representation*:

$$\mathbf{P}_{\mathbf{G}}^{(\mathbf{x}\mathbf{x})} = \mathbf{P}_{\mathbf{G}}^{(\mathbf{x})} \oplus \mathbf{P}_{\mathbf{G}}^{(\mathbf{x})} = \{\mathbf{P}_g^{(\mathbf{x})} \oplus \mathbf{P}_g^{(\mathbf{x})} \mid \forall g \in \mathbf{G}\}, \quad (25)$$

where the symbol $\mathbf{P}_g^{(\mathbf{x})} \oplus \mathbf{P}_g^{(\mathbf{x})}$ is a combination of the two permutations for g at issue.

The degree of the combined representation (Eq. 25) is equal to $n + 2$.

The combined representation (Eq. 25) can be regarded as a permutation group isomorphic (or generally homomorphic) to the original *RS*-stereoisomeric group \mathbf{G} . For example, the *RS*-stereoisomeric group $\mathbf{T}_{d\tilde{\sigma}\hat{I}}$ for characterizing the total feature of Figure 1 can be constructed by using the `Group` function of the GAP system, where a set of generators (the argument of the function `Group` of `TdsI`) is composed of (1,3)(2,4) for a two-fold rotation, (2,3,4) for a three-fold rotation, (1,3)(5,6) for a reflection, and (5,6) for a ligand reflection. Note that (5,6) corresponds to \hat{I} . The commands of the GAP system and their results are shown in the $\mathbf{T}_{d\tilde{\sigma}\hat{I}}$ -part (the fifth part) of Table 1.

2.6 Properties of *RS*-Stereoisomeric Groups

2.6.1 Selection of Sets of Generators

To select a set of generators for constructing an *RS*-stereoisomeric group, there are three modes as follows:

1. The first mode of selection is the addition of a ligand reflection to a set of generators for constructing the point group $\overline{\mathbf{G}}$. This mode reflects the coset decomposition of \mathbf{G} by $\overline{\mathbf{G}}$:

$$\mathbf{G} = (\mathbf{G}^{(m)} + \mathbf{G}^{(m)}\sigma) + (\mathbf{G}^{(m)}\tilde{\sigma} + \mathbf{G}^{(m)}\hat{I}) = \overline{\mathbf{G}} + \overline{\mathbf{G}}\hat{I}, \quad (26)$$

which is obtained by starting from Eq. 19.

For example, the construction of $\mathbf{T}_{d\tilde{\sigma}\hat{I}}$ (`TdsI`) shown in Table 1 stems from the addition of the ligand reflection (5,6) to the point group \mathbf{T}_d (`Td`). This aims at emphasizing the extension of the point group \mathbf{T}_d to the *RS*-stereoisomeric group $\mathbf{T}_{d\tilde{\sigma}\hat{I}}$. Note that chirality under a point group $\overline{\mathbf{G}}$ (e.g., \mathbf{T}_d) is regarded as a kind of handedness in general, where a pair of attributes, i.e., chirality/achirality, is provided according to the vertical direction of a stereoisogram (e.g., Figure 1).

2. The second mode of selection is the addition of a ligand reflection to a set of generators for constructing the *RS*-permutation group $\tilde{\mathbf{G}}$. Thus, an alternative con-

struction is possible by adding the ligand reflection (5,6) to the *RS*-permutation group $\mathbf{T}_{\tilde{\sigma}} (\mathbf{Ts})$, i.e., $\mathbf{TdsI} := \text{Group}([(1,3)(2,4), (2,3,4), (1,3), (5,6)])$. This generation more clearly supports the coset decomposition (Eq. 20) because of $\tilde{\mathbf{G}}\sigma = \tilde{\mathbf{G}}\hat{I}$ (e.g., $\mathbf{T}_{\tilde{\sigma}}\sigma = \mathbf{T}_{\tilde{\sigma}}\hat{I}$). Note that *RS*-stereogenicity under an *RS*-permutation group $\tilde{\mathbf{G}}$ (e.g., $\mathbf{T}_{\tilde{\sigma}}$) is regarded as another kind of handedness, where a pair of attributes, i.e., *RS*-stereogenicity/*RS*-astereogenicity, is provided according to the horizontal direction of a stereoisogram (e.g., Figure 1). This mode of construction provides us with an alternative formulation of *RS*-stereoisomeric groups.

3. The third mode is to select a set of generators, which can be considered to be generated by the addition of an *RS*-permutation to a set of generators for constructing the point group $\overline{\mathbf{G}}$ as well as the addition of a reflection to a set of generators for constructing the *RS*-permutation group $\tilde{\mathbf{G}}$. As a result, such a selected set of generators does not contain a permutation for a ligand reflection. Thus, a further set of generators $[(1,3)(2,4), (2,3,4), (1,3)(5,6), (1,3)]$ also generates the *RS*-stereoisomeric group $\mathbf{T}_{d\tilde{\sigma}\hat{I}}$. This set of generators can be considered to be the addition of an *RS*-permutation (1,3) to the point group $\mathbf{T}_d (\mathbf{Td})$ as well as the addition of a reflection (1,3)(5,6) to the *RS*-permutation group $\mathbf{T}_{\tilde{\sigma}} (\mathbf{Ts})$. Although a ligand reflection is not contained in the set of generators, it is generated by a subsequent multiplication such as $\sigma\tilde{\sigma} = \hat{I}$ (e.g., $(1,3)(5,6)^*(1,3) = (5,6)$). This multiplication corresponds to the diagonal direction which links $\mathbf{2}$ and $\overline{\mathbf{1}}$ in Figure 1 (note $\overline{(1)(2\ 4)(3)} * (1)(2\ 4)(3) = \overline{(1)(2)(3)(4)}$).

2.6.2 Subgroups of *RS*-Stereoisomeric Groups

The *RS*-Stereoisomeric group \mathbf{G} is decomposed into a set of cosets represented by Eq. 19, where the maximum chiral subgroup $\mathbf{G}^{(m)}$ is a normal subgroup. The coset decomposition of the *RS*-stereoisomeric group $\mathbf{T}_{d\tilde{\sigma}\hat{I}}$ by \mathbf{T} is represented as follows:

$$\mathbf{T}_{d\tilde{\sigma}\hat{I}} = \mathbf{T} + \mathbf{T}\sigma + \mathbf{T}\tilde{\sigma} + \mathbf{T}\hat{I}. \quad (27)$$

When the combined representation of $\mathbf{T}_{d\tilde{\sigma}\hat{I}} (\mathbf{TdsI})$ is regarded as a permutation group (Table 1), the coset decomposition of $\mathbf{T}_{d\tilde{\sigma}\hat{I}} (\mathbf{TdsI})$ by the subgroup $\mathbf{T} (\mathbf{T})$ is calculated as a list of cosets (`1_cosets`) by using the function `CosetDecomposition` of the GAP system:

```

gap> l_cosets := CosetDecomposition(TdsI, T);;
gap> Print("TdsI= $\cup$ T $\cup$ T*s $\cup$ T*I $\cup$ T*d: $\cup$ \n", l_cosets, "\n");
TdsI = T + T*s + T*I + T*d:
[ [ (0, (2,3,4), (2,4,3), (1,2)(3,4), (1,2,3), (1,2,4), (1,3,2), (1,3,4), (1,3)(2,4), (1,4,2),
    (1,4,3), (1,4)(2,3) ],
  [ (3,4), (2,4), (2,3), (1,2), (1,2,4,3), (1,2,3,4), (1,4,3,2), (1,4), (1,4,2,3), (1,3,4,2),
    (1,3), (1,3,2,4) ],
  [ (5,6), (2,3,4)(5,6), (2,4,3)(5,6), (1,2)(3,4)(5,6), (1,2,3)(5,6), (1,2,4)(5,6), (1,3,2)(5,6),
    (1,3,4)(5,6), (1,3)(2,4)(5,6), (1,4,2)(5,6), (1,4,3)(5,6), (1,4)(2,3)(5,6) ],
  [ (3,4)(5,6), (2,4)(5,6), (2,3)(5,6), (1,2)(5,6), (1,2,4,3)(5,6), (1,2,3,4)(5,6), (1,4,3,2)(5,6),
    (1,4)(5,6), (1,4,2,3)(5,6), (1,3,4,2)(5,6), (1,3)(5,6), (1,3,2,4)(5,6) ] ]

```

The resulting list (`l_cosets`) is composed of four inner lists, each of which is surrounded in a pair of square brackets. They correspond respectively to \mathbf{T} (`l_cosets[1]`), $\mathbf{T}\tilde{\sigma}$ (`l_cosets[2]`), $\mathbf{T}\hat{I}$ (`l_cosets[3]`), and $\mathbf{T}\sigma$ (`l_cosets[4]`). This is confirmed, for example, by constructing `l_Tdtemp` (for \mathbf{T}_d) by summing up `l_cosets[1]` (for \mathbf{T}) and `l_cosets[4]` (for $\mathbf{T}\sigma$). The sum `l_Tdtemp` is shown to be an equal set to `element_Td` calculated above for the point group \mathbf{T}_d (\mathbf{T}_d) (Table 1), as confirmed by using the function `IsEqualSet` of the GAP system:

```

gap> l_Tdtemp := Concatenation(l_cosets[1], l_cosets[4]);;
gap> Print("Td: $\cup$ ", l_Tdtemp, "\n");
Td: [ (0, (2,3,4), (2,4,3), (1,2)(3,4), (1,2,3), (1,2,4), (1,3,2), (1,3,4), (1,3)(2,4), (1,4,2), (1,4,3),
    (1,4)(2,3), (3,4)(5,6), (2,4)(5,6), (2,3)(5,6), (1,2)(5,6), (1,2,4,3)(5,6), (1,2,3,4)(5,6),
    (1,4,3,2)(5,6), (1,4)(5,6), (1,4,2,3)(5,6), (1,3,4,2)(5,6), (1,3,4)(5,6), (1,3,2,4)(5,6) ]
gap> Print("Td_OK?: $\cup$ ", IsEqualSet(element_Td, l_Tdtemp), "\n");
Td_OK?: true

```

In a similar way, the summation of `l_cosets[1]` and `l_cosets[2]` produces an equal set to `Ts` for the *RS*-permutation group $\mathbf{T}_{\tilde{\sigma}}$, while the summation of `l_cosets[1]` and `l_cosets[3]` produces an equal set to `TI` for the ligand-reflection group $\mathbf{T}_{\hat{I}}$.

2.6.3 Conjugacy Classes of *RS*-Stereoisomeric Groups

The comparison between the coset decomposition of the point group $\overline{\mathbf{G}}$ (Eq. 2) and that of the *RS*-stereoisomeric group \mathbf{G} (Eq. 20) indicates the parallelism of their group structures. It follows that the GAP function `divideConjClasses` developed for calculating a list of conjugacy classes of a point group $\overline{\mathbf{G}}$ [43] can be applied, as it is, to an *RS*-stereoisomeric group \mathbf{G} .

Because the source list of the function `divideConjClasses` is stored in the file named `CICFgenCC.func` (Appendix A of [43]), the file is beforehand loaded by means of the GAP command `Read`. Thereby, the following result of the *RS*-stereoisomeric group $\mathbf{T}_{d\hat{\sigma}\hat{I}}$ (`TdsI`) is obtained:

```

gap> Read("c:/fujita0/fujita2016/TdsI-GAP/Calc-GAP/CICFgenCC.gapfunc");
gap> gen1 := [(1,3)(2,4), (2,3,4), (1,3)(5,6), (5,6)];;
gap> TdsI := Group(gen1);
Group([ (1,3)(2,4), (2,3,4), (1,3)(5,6), (5,6) ])
gap> l_conjclass := divideConjClasses(TdsI, 4, 6);
[ [ [ (0) ], [ (3,4), (2,3), (2,4), (1,2), (1,3), (1,4) ],

```

```
[ (2,3,4), (2,4,3), (1,2,3), (1,2,4), (1,3,2), (1,3,4), (1,4,2), (1,4,3) ],
[ (1,2)(3,4), (1,3)(2,4), (1,4)(2,3) ],
[ (1,2,3,4), (1,2,4,3), (1,3,4,2), (1,3,2,4), (1,4,3,2), (1,4,2,3) ] ],
[ (5,6) ], [ (3,4)(5,6), (2,3)(5,6), (2,4)(5,6), (1,2)(5,6), (1,3)(5,6), (1,4)(5,6) ],
[ (2,3,4)(5,6), (2,4,3)(5,6), (1,2,3)(5,6), (1,2,4)(5,6), (1,3,2)(5,6), (1,3,4)(5,6), (1,4,2)(5,6),
  (1,4,3)(5,6) ],
[ (1,2)(3,4)(5,6), (1,3)(2,4)(5,6), (1,4)(2,3)(5,6) ],
[ (1,2,3,4)(5,6), (1,2,4,3)(5,6), (1,3,4,2)(5,6), (1,3,2,4)(5,6), (1,4,3,2)(5,6), (1,4,2,3)(5,6) ] ] ]
```

The resulting list named `l_conjclass` contains two inner lists `l_conjclass[1]` and `l_conjclass[2]` according to the following coset decomposition:

$$\mathbf{T}_{d\hat{\sigma}\hat{\Gamma}} = \mathbf{T}_{\hat{\sigma}} + \mathbf{T}_{\hat{\sigma}\sigma} \tag{28}$$

where the first list `l_conjclass[1]` consists of five conjugacy classes of $\mathbf{T}_{\hat{\sigma}}$ (without (5,6)), while the second list `l_conjclass[2]` consists of five conjugacy classes of $\mathbf{T}_{\hat{\sigma}\sigma}$ (with (5,6)). Thus, the elements of $\mathbf{T}_{d\hat{\sigma}\hat{\Gamma}}$ listed in the last part of Table 1 are classified into totally ten conjugacy classes. Note that each conjugacy class contains permutations (products of cycles) having the same cycle structure.

2.6.4 Point Groups Isomorphic to *RS*-Stereoisomeric Groups

The parallelism between the point group $\overline{\mathbf{G}}$ (cf. Eq. 2) and the *RS*-stereoisomeric group \mathbf{G} (cf. Eq. 20) means that there may be a point group isomorphic to the *RS*-stereoisomeric group \mathbf{G} . For example, the *RS*-stereoisomeric group $\mathbf{T}_{d\hat{\sigma}\hat{\Gamma}}$ (order 48) has been demonstrated to be isomorphic to the point group \mathbf{O}_h (order 48) [29]. These two groups are parallel with respect to their coset decompositions. Compare the coset decomposition of $\mathbf{T}_{d\hat{\sigma}\hat{\Gamma}}$ (Eq. 28) with the following coset decomposition of \mathbf{O}_h :

$$\mathbf{O}_h = \mathbf{O} + \mathbf{O}\sigma, \tag{29}$$

where the symbol \mathbf{O} denotes the maximum chiral subgroup of \mathbf{O}_h .

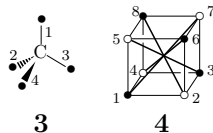


Figure 2. A reference tetrahedral skeleton **3** and a reference cubic skeleton **4**

The parallelism between $\mathbf{T}_{d\hat{\sigma}\hat{\Gamma}}$ and \mathbf{O}_h can be confirmed by comparing `TdsI` generated from a set of generators:

$$\text{gen1} = [(1,3)(2,4), (2,3,4), (1,3)(5,6), (5,6)]$$

with Oh_cube generated from a set of generators:

$$\begin{aligned} \text{gen2} := & [(1,3)(2,4)(5,7)(6,8), (2,4,5)(3,8,6), \\ & (1,3)(5,7)(9,10), (1,7)(2,8)(3,5)(4,6)(9,10)]. \end{aligned}$$

Although the point group \mathbf{O}_h (Oh_cube) has been generated from a different set of generators in a previous paper [43], the adoption of the above sets of generators gen1 and gen2 is convenient to trace the correspondence between a tetrahedral skeleton $\mathbf{3}$ and a cubic skeleton $\mathbf{4}$ (Figure 2).

The equivalent eight vertices of the cube $\mathbf{4}$ are classified into two sets (with an open circle and a solid circle), so that the vertices with a solid circle is correlated to the four vertices of the tetrahedron $\mathbf{3}$. Thereby, the correspondence between gen1 and gen2 are interpreted visually. Thus, the generator $(1,3)(2,4)(5,7)(6,8)$ of gen2 corresponds to a two-fold rotation running through the centers of the top and bottom faces of $\mathbf{4}$, so that it is correlated to the generator $(1,3)(2,4)$ of gen1 . The generator $(2,4,5)(3,8,6)$ of gen2 corresponds to a three-fold rotation running through vertices 1 and 7 of $\mathbf{4}$, so that it is correlated to the generator $(2,3,4)$ of gen1 . The generator $(1,3)(5,7)(9,10)$ of gen2 corresponds to a reflection concerning the mirror plane 2–4–8–6 of $\mathbf{4}$, so that it is correlated to the generator $(1,3)(5,6)$ of gen1 . The last generator $(1,7)(2,8)(3,5)(4,6)(9,10)$ corresponds to an inversion at the center of the cube $\mathbf{4}$, so that it is correlated to a ligand reflection \hat{I} , which is represented by $(5,6)$ of gen1 .

The correspondence between the elements of $\mathbf{T}_{d\bar{\sigma}I}$ and those of \mathbf{O}_h is calculated by using the following source list stored in the file named `TdsI-Oh6.gap` tentatively.

```
#Read("c:/fujita0/fujita2016/TdsI-GAP/calc-GAP/TdsI-Oh6.gap");
LogTo("c:/fujita0/fujita2016/TdsI-GAP/calc-GAP/TdsI-Oh6log.txt");

Read("c:/fujita0/fujita2016/TdsI-GAP/calc-GAP/CICFgenCC.gapfunc");

gen1 := [(1,3)(2,4), (2,3,4), (1,3)(5,6), (5,6)];
TdsI := Group(gen1); #TdsI
gen2 := [(1,3)(2,4)(5,7)(6,8), (2,4,5)(3,8,6), (1,3)(5,7)(9,10), (1,7)(2,8)(3,5)(4,6)(9,10)];
Oh_cube := Group(gen2); #cube

l_conjclass := divideConjClasses(TdsI, 4, 6);
l1_conjclass := l_conjclass[1]; l2_conjclass := l_conjclass[2];

hom1 := GroupHomomorphismByImages(TdsI, Oh_cube, gen1, gen2);

for j in [1..Size(l1_conjclass)] do
l11 := l1_conjclass[j];
for i in [1..Size(l11)] do
Print(l11[i], "%", Image(hom1, l11[i]), "\\\n");
od; Print("\\hline\n"); od;
Print("\\hline\n");
```

```

for j in [1..Size(l2_conjclass)] do
l12 := l2_conjclass[j];
for i in [1..Size(l12)] do
Print(l12[i], "&", Image(hom1, l12[i]), "\\\n\n");
od; Print("\\hline\n"); od;
LogTo();

```

When inputting this file to the GAP system, the respective commands are successively executed. The elements of $\mathbf{T}_{d\hat{\sigma}\hat{\tau}}$ are beforehand classified into conjugacy classes as described above (the function `divideConjClasses`). Then, the correspondence between the elements of $\mathbf{T}_{d\hat{\sigma}\hat{\tau}}$ and those of \mathbf{O}_h are calculated by means of the GAP functions `GroupHomomorphismByImages` and `Image`. The calculated data are stored in the log file named `TdsI-0h6log.txt` tentatively. They are summarized in a tabular form to give Table 2, where each row with an asterisk indicates the correspondence between `gen1` and `gen2`.

The permutations of the $\mathbf{T}_{d\hat{\sigma}\hat{\tau}}$ -column and those of the \mathbf{O}_h -column in Table 2 can be correlated diagrammatically by comparing **3** and **4** of Figure 2. Let us examine, for example, the correspondence between (3,4) for **3** and (1, 7)(2, 3)(4, 6)(5, 8) for **4** (the second row of Table 2). The set of four diagonal lines (boldfaced) of the cube **4** is considered as an ordered set as follows:

$$\{\text{line 1-7 } (\bullet\text{-}\circ), \text{line 6-4 } (\bullet\text{-}\circ), \text{line 3-5 } (\bullet\text{-}\circ), \text{line 8-2 } (\bullet\text{-}\circ)\} = \{1, 2, 3, 4\}, \quad (30)$$

where the four diagonal lines are numbered sequentially. Although the terminals of each line are tentatively differentiated by an open circle and a solid circle, they are equivalent under the action of \mathbf{O}_h . The permutation (1, 7)(2, 3)(4, 6)(5, 8), which corresponds to a two-fold rotation through the midpoints of edges 2-3 and 5-8 in the cube **4**, acts on the ordered set so as to give another ordered set:

$$\begin{aligned} \{\text{line 7-1 } (\circ\text{-}\bullet), \text{line 4-6 } (\circ\text{-}\bullet), \text{line 2-8 } (\circ\text{-}\bullet), \text{line 5-3 } (\circ\text{-}\bullet)\} &= \\ \{\text{line 1-7 } (\bullet\text{-}\circ), \text{line 6-4 } (\bullet\text{-}\circ), \text{line 8-2 } (\bullet\text{-}\circ), \text{line 3-5 } (\bullet\text{-}\circ)\} &= \{1, 2, 4, 3\}. \end{aligned} \quad (31)$$

This action (from Eq. 30 to Eq. 31) is represented by the following permutation:

$$\begin{pmatrix} 1 & 2 & 3 & 4 \\ 1 & 2 & 4 & 3 \end{pmatrix} = (1)(2)(3\ 4) = (3\ 4), \quad (32)$$

which is equal to the (3,4) for **3**. In other words, the four diagonal lines of **4** (Eq. 30) corresponds to the four vertices of **3**.

Table 2. Correspondence between $T_{d\hat{\sigma}\hat{I}}$ for a tetrahedron and O_h for a cube

$T_{d\hat{\sigma}\hat{I}}$ for a tetrahedron TdsI := Group(gen1) $P_{T_{d\hat{\sigma}\hat{I}}}^{(X)}$	O_h for a cube Oh.cube := Group(gen2) $P_{O_h\text{-cube}}^{(X)}$
()	()
(3,4)	(1, 7)(2, 3)(4, 6)(5, 8)
(2,3)	(1, 7)(2, 8)(3, 4)(5, 6)
(2,4)	(1, 7)(2, 6)(3, 5)(4, 8)
(1,2)	(1, 4)(2, 8)(3, 5)(6, 7)
(1,3)	(1, 5)(2, 8)(3, 7)(4, 6)
(1,4)	(1, 2)(3, 5)(4, 6)(7, 8)
(2,3,4)*	(2, 4, 5)(3, 8, 6)
(2,4,3)	(2, 5, 4)(3, 6, 8)
(1,2,3)	(1, 6, 3)(4, 5, 7)
(1,2,4)	(1, 6, 8)(2, 7, 4)
(1,3,2)	(1, 3, 6)(4, 7, 5)
(1,3,4)	(1, 3, 8)(2, 7, 5)
(1,4,2)	(1, 8, 6)(2, 4, 7)
(1,4,3)	(1, 8, 3)(2, 5, 7)
(1,2)(3,4)	(1, 6)(2, 5)(3, 8)(4, 7)
(1,3)(2,4)*	(1, 3)(2, 4)(5, 7)(6, 8)
(1,4)(2,3)	(1, 8)(2, 7)(3, 6)(4, 5)
(1,2,3,4)	(1, 4, 3, 2)(5, 8, 7, 6)
(1,2,4,3)	(1, 4, 8, 5)(2, 3, 7, 6)
(1,3,4,2)	(1, 5, 8, 4)(2, 6, 7, 3)
(1,3,2,4)	(1, 5, 6, 2)(3, 4, 8, 7)
(1,4,3,2)	(1, 2, 3, 4)(5, 6, 7, 8)
(1,4,2,3)	(1, 2, 6, 5)(3, 7, 8, 4)
(5,6)*	(1, 7)(2, 8)(3, 5)(4, 6)(9,10)
(3,4)(5,6)	(2, 5)(3, 8)(9,10)
(2,3)(5,6)	(3, 6)(4, 5)(9,10)
(2,4)(5,6)	(2, 4)(6, 8)(9,10)
(1,2)(5,6)	(1, 6)(4, 7)(9,10)
(1,3)(5,6)*	(1, 3)(5, 7)(9,10)
(1,4)(5,6)	(1, 8)(2, 7)(9,10)
(2,3,4)(5,6)	(1, 7)(2, 6, 5, 8, 4, 3)(9,10)
(2,4,3)(5,6)	(1, 7)(2, 3, 4, 8, 5, 6)(9,10)
(1,2,3)(5,6)	(1, 4, 3, 7, 6, 5)(2, 8)(9,10)
(1,2,4)(5,6)	(1, 4, 8, 7, 6, 2)(3, 5)(9,10)
(1,3,2)(5,6)	(1, 5, 6, 7, 3, 4)(2, 8)(9,10)
(1,3,4)(5,6)	(1, 5, 8, 7, 3, 2)(4, 6)(9,10)
(1,4,2)(5,6)	(1, 2, 6, 7, 8, 4)(3, 5)(9,10)
(1,4,3)(5,6)	(1, 2, 3, 7, 8, 5)(4, 6)(9,10)
(1,2)(3,4)(5,6)	(1, 4)(2, 3)(5, 8)(6, 7)(9,10)
(1,3)(2,4)(5,6)	(1, 5)(2, 6)(3, 7)(4, 8)(9,10)
(1,4)(2,3)(5,6)	(1, 2)(3, 4)(5, 6)(7, 8)(9,10)
(1,2,3,4)(5,6)	(1, 6, 3, 8)(2, 7, 4, 5)(9,10)
(1,2,4,3)(5,6)	(1, 6, 8, 3)(2, 5, 7, 4)(9,10)
(1,3,4,2)(5,6)	(1, 3, 8, 6)(2, 4, 7, 5)(9,10)
(1,3,2,4)(5,6)	(1, 3, 6, 8)(2, 7, 5, 4)(9,10)
(1,4,3,2)(5,6)	(1, 8, 3, 6)(2, 5, 4, 7)(9,10)
(1,4,2,3)(5,6)	(1, 8, 6, 3)(2, 4, 5, 7)(9,10)

3 Enumeration Under *RS*-Stereoisomeric Groups

3.1 CI-CFs for *RS*-Stereoisomeric Groups

For the purpose of gross enumeration of 3D structures, Fujita's proligrand method [35–38] adopts the concept of *sphericities of cycles*, i.e., homospheric, enantiospheric, and hemispheric cycles, during the action of point groups $\overline{\mathbf{G}}$. This concept has been extended to cover the effect of *RS*-stereoisomeric groups \mathbf{G} (Eq. 11 of [39]). The extended CI-CF should be further modified from the present viewpoint, so as to be harmonized with the combined-permutation representation $\mathbf{P}_G^{(\mathbf{x}\mathbf{x})}$ (Eq. 25).

Let us focus our attention on a k -cycle in a given product of cycles which is contained in the $\mathbf{P}_G^{(\mathbf{x})}$ -part of $\mathbf{P}_G^{(\mathbf{x}\mathbf{x})}$ (Eq. 25). A k -cycle contained in a product of cycles for g ($\in \tilde{\mathbf{G}} \subset \mathbf{G}$) which exhibits a mirror-coset representation $\mathbf{P}_g^{(\mathbf{x})} = (n+1)(n+2)$ (for $\forall g \in \tilde{\mathbf{G}}$ in Eq. 23) is referred to as a *hemispheric cycle* and characterized by a sphericity index b_k . On the other hand, a k -cycle contained in a product of cycles for g ($\in \tilde{\mathbf{G}}\sigma \subset \mathbf{G}$) which exhibits a mirror-coset representation $\mathbf{P}_g^{(\mathbf{x})} = (n+1 \ n+2)$ (for $\forall g \in \tilde{\mathbf{G}}\sigma$ in Eq. 24) is categorized into a homospheric cycle (sphericity index: a_k) if k is odd or an enantiospheric cycle (sphericity index: c_k) if k is even.

Suppose that an element $\mathbf{P}_g^{(\mathbf{x})}$ of degree n (cf. Eq. 25) is represented by a cycle decomposition involving the number $\nu_k(\mathbf{P}_g^{(\mathbf{x})})$ of k -cycles ($\sum_{k=1}^n k\nu_k(\mathbf{P}_g^{(\mathbf{x})})$). Then the element $\mathbf{P}_g^{(\mathbf{x}\mathbf{x})}$ corresponding to $\mathbf{P}_g^{(\mathbf{x})}$ (cf. Eq. 25) is specified by a product of sphericity indices (PSI):

$$\text{PSI}_{\mathbf{P}_g^{(\mathbf{x}\mathbf{x})}} = \mathbb{S}_1^{\nu_1(\mathbf{P}_g^{(\mathbf{x})})} \mathbb{S}_2^{\nu_2(\mathbf{P}_g^{(\mathbf{x})})} \dots \mathbb{S}_n^{\nu_n(\mathbf{P}_g^{(\mathbf{x})})}, \quad (33)$$

where \mathbb{S}_k is a_k if $\mathbf{P}_g^{(\mathbf{x})} = (n+1 \ n+2)$ (one 2-cycle) and k is odd; \mathbb{S}_k is c_k if $\mathbf{P}_g^{(\mathbf{x})} = (n+1 \ n+2)$ (one 2-cycle) and k is even; and \mathbb{S}_k is b_k if $\mathbf{P}_g^{(\mathbf{x})} = (n+1)(n+2)$ (two 1-cycles). According to Def. 7.20 of [38], the cycle index with chirality fittingness (CI-CF) for $\mathbf{P}_G^{(\mathbf{x}\mathbf{x})}$ is calculated as follows by using the PSIs (Eq. 33):

$$\text{CI-CF}(\mathbf{P}_G^{(\mathbf{x}\mathbf{x})}; \mathbb{S}_k) = \frac{1}{|\mathbf{G}|} \sum_{g \in \mathbf{G}} \mathbb{S}_1^{\nu_1(\mathbf{P}_g^{(\mathbf{x})})} \mathbb{S}_2^{\nu_2(\mathbf{P}_g^{(\mathbf{x})})} \dots \mathbb{S}_n^{\nu_n(\mathbf{P}_g^{(\mathbf{x})})}. \quad (34)$$

Note that any permutation of the conjugacy class $\text{Cl}(g)$ has the same mode of cycle decomposition, or equivalently the same cycle structure. This means that $\text{PSI}_{\mathbf{P}_g^{(\mathbf{x}\mathbf{x})}}$ (Eq. 33) is common to all of the element $g \in \text{Cl}(g)$, so that the PSI for the conjugacy class

$\text{Cl}(g)$ can be written as follows:

$$\text{PSI}_{\mathbf{P}_{\text{Cl}(g)}^{(\mathbf{x})}} = \mathfrak{S}_1^{\nu_1(\mathbf{P}_{\text{Cl}(g)}^{(\mathbf{x})})} \mathfrak{S}_2^{\nu_2(\mathbf{P}_{\text{Cl}(g)}^{(\mathbf{x})})} \dots \mathfrak{S}_n^{\nu_n(\mathbf{P}_{\text{Cl}(g)}^{(\mathbf{x})})}. \quad (35)$$

Thereby, the CI-CF (Eq. 34) for $\mathbf{P}_{\mathbf{G}}^{(\mathbf{x})}$ is rewritten as follows:

$$\text{CI-CF}(\mathbf{P}_{\mathbf{G}}^{(\mathbf{x})}; \mathfrak{S}_k) = \frac{1}{|\mathbf{G}|} \sum_{\text{Cl}(g)} |\text{Cl}(g)| \mathfrak{S}_1^{\nu_1(\mathbf{P}_{\text{Cl}(g)}^{(\mathbf{x})})} \mathfrak{S}_2^{\nu_2(\mathbf{P}_{\text{Cl}(g)}^{(\mathbf{x})})} \dots \mathfrak{S}_n^{\nu_n(\mathbf{P}_{\text{Cl}(g)}^{(\mathbf{x})})}, \quad (36)$$

where the summation concerning $\text{Cl}(g)$ runs to cover the representatives of the conjugacy classes contained in \mathbf{G} and the symbol $|\text{Cl}(g)|$ represents the size of the corresponding conjugacy class $\text{Cl}(g)$.

3.2 Calculation of CI-CFs

The parallelism between the point group $\overline{\mathbf{G}}$ (cf. Eq. 2) and the *RS*-stereoisomeric group \mathbf{G} (cf. Eq. 20) means that the cycle index with chirality fittingness (CI-CF) for \mathbf{G} can be calculated in a similar way to $\overline{\mathbf{G}}$. It follows that a function for calculating the CI-CF of the point group $\overline{\mathbf{G}}$ is applicable to the calculation of the CI-CF of the *RS*-stereoisomeric group \mathbf{G} .

A function `CalcCICF` has been developed as a GAP function for calculating CI-CFs under point groups [42]. The function `CalcCICF` is applicable to calculate CI-CFs (Eq. 34) under *RS*-stereoisomeric groups. Another function `CalcConjClassCICF` for calculating CI-CFs under point groups has also been developed [43], where conjugacy classes are taken into consideration. The function `CalcConjClassCICF` is applicable to calculate CI-CFs (Eq. 36) under *RS*-stereoisomeric groups. These two functions are capable of bringing about equal CI-CFs.

Because the source list of the function `CalcConjClassCICF` is stored in the file named `CICFgenCC.func` (Appendix A of [43]), the file is beforehand loaded by means of the GAP command `Read`. The application of the function `CalcConjClassCICF` to the calculation of the CI-CF (`CICF_TdsI`) of the *RS*-stereoisomeric group $\mathbf{T}_{d\overline{\sigma}I}$ is executed as follows:

```
gap> Read("c:/fujita0/fujita2016/TdsI-GAP/calC-GAP/CICFgenCC.gapfunc");
gap> gen_1 := [(1,3)(2,4), (2,3,4), (1,3)(5,6), (5,6)];;
gap> TdsI := Group(gen_1);
Group([(1,3)(2,4), (2,3,4), (1,3)(5,6), (5,6) ])
gap> CICF_TdsI := CalcConjClassCICF(TdsI, 4, 6);
1/48*b_1^4+1/48*a_1^4+1/8*b_1^2*b_2+1/8*a_1^2*c_2+1/6*b_1*b_3+1/6*a_1*a_3+1/16*b_2^2+1/16*c_2^2+1/8*b_4
  ↪ +1/8*c_4
```

The resulting CI-CF (`CICF_TdsI`) is confirmed by examining the cycle structures of each term collected in the $\mathbf{T}_{d\overline{\sigma}I}$ -column of Table 2. According to Fujita's proligand method

[35], the identity element $()$ means $(1)(2)(3)(4)$ so as to provide a product of sphericity indices (PSI) b_1^4 , six elements of a 2-cycle (e.g., $(3,4)$ meaning $(1)(2)(3\ 4)$) provide a PSI $6*b_1^2*b_2$ ($6b_1^2b_2$), eight elements of a 3-cycle (e.g., $(2,3,4)$) provide a PSI $8*b_1*b_3$ ($8b_1b_3$), three elements of two 2-cycles (e.g., $(1,2)(3,4)$) provide a PSI $3*b_2^2$ ($3b_2^2$), and six elements of a 4-cycle (e.g., $(1,2,3,4)$) provide a PSI $6*b_4$ ($6b_4$). Each element with $(5,6)$ corresponds to a (roto)reflection or a ligand reflection, which is represented by an overline, as described above. Thus, one element $(5,6)$ means $(1)(2)(3)(4)$ so as to provide a PSI a_1^4 , six elements of a 2-cycle with $(5,6)$ (e.g., $(3,4)(5,6)$ meaning $(1)(2)(3\ 4)$) provide a PSI $6*a_1^2*c_2$ ($6a_1^2c_2$), eight elements of a 3-cycle with $(5,6)$ (e.g., $(2,3,4)(5,6)$) provide a PSI $8*a_1*a_3$ ($8a_1a_3$), three elements of two 2-cycles with $(5,6)$ (e.g., $(1,2)(3,4)(5,6)$) provide a PSI $3*c_2^2$ ($3c_2^2$), and six elements of a 4-cycle with $(5,6)$ (e.g., $(1,2,3,4)(5,6)$) provide a PSI $6*c_4$ ($6c_4$). These PSIs are summed up and divided by the order of $T_{d\bar{\sigma}\hat{f}}$ (48) to give the CI-CF of $T_{d\bar{\sigma}\hat{f}}$. The resulting CI-CF is identical with the C1cConjClassCICF calculated above.

The procedure based on the function CalcConjClassCICF for calculating a CI-CF can be applied to the groups listed in Table 1. The calculated CI-CFs for the groups are collected in Table 3. The format of each term of the resulting CI-CFs obeys the GAP notation. Thus, the symbol $*$ represents a multiplication and the symbol \wedge represent a power. The CI-CFs listed in Table 3 are consistent with the CI-CFs reported previously (Eqs. 64–68 of [39] and Eqs. 58–62 of [40]), which have been calculated by an alternative procedure without relying on the present computer-oriented representations.

3.3 Enumeration of Tetrahedral Derivatives

Suppose that the four positions of a tetrahedral skeleton **1** (or **3**) accommodate a set of four proligands selected from a given ligand inventory:

$$L = \{A, B, C, D; p, \bar{p}, q, \bar{q}, r, \bar{r}, s, \bar{s}\}, \quad (37)$$

where the uppercase letters A, B, C, and D represent achiral proligands, while a pair of lowercase letters p/\bar{p} , q/\bar{q} , r/\bar{r} , or s/\bar{s} represents an enantiomeric pair of chiral proligands in isolation. Theorem 7.14 of [38] for the point group is applied to the present case under the *RS*-stereoisomeric group $T_{d\bar{\sigma}\hat{f}}$. Thereby, the sphericity indices ($\$k$: a_k , c_k , and b_k)

Table 3. CI-CFs of *RS*-Stereoisomeric Group $T_{d\bar{\sigma}\bar{\Gamma}}$ and its Subgroups for Characterizing a Tetrahedral Skeleton

group	a list of generators, CI-CF
T_d (point group)	Td:= Group([(1,3)(2,4), (2,3,4), (1,3)(5,6)]) CICF_Td := 1/24*b_1^4+1/4*a_1^2*c_2+1/3*b_1*b_3+1/8*b_2^2+1/4*c_4
$T_{\bar{\sigma}}$ (<i>RS</i> -permutation group)	Ts:= Group([(1,3)(2,4), (2,3,4), (1,3)]) CICF_Ts := 1/24*b_1^4+1/4*b_1^2*b_2+1/3*b_1*b_3+1/8*b_2^2+1/4*b_4
$T_{\bar{\Gamma}}$ (ligand-reflection group)	TI:= Group([(1,3)(2,4), (2,3,4), (5,6)]) CICF_TI := 1/24*b_1^4+1/24*a_1^4+1/3*b_1*b_3+1/3*a_1*a_3 +1/8*c_2^2+1/8*b_2^2
T (normal subgroup)	T:= Group([(1,3)(2,4), (2,3,4)]) CICF_T := 1/12*b_1^4+2/3*b_1*b_3+1/4*b_2^2
$T_{d\bar{\sigma}\bar{\Gamma}}$ (<i>RS</i> -stereoisomeric group)	TdsI:= Group([(1,3)(2,4), (2,3,4), (1,3)(5,6), (5,6)]) CICF_TdsI := 1/48*b_1^4+1/48*a_1^4+1/8*b_1^2*b_2+1/8*a_1^2*c_2 +1/6*b_1*b_3+1/6*a_1*a_3+1/16*c_2^2+1/16*b_2^2+1/8*c_4+1/8*b_4

contained in the CI-CFs are substituted by the following ligand-inventory functions:

$$a_k = A^k + B^k + C^k + D^k \quad (38)$$

$$c_k = A^k + B^k + C^k + D^k + 2p^{k/2}\bar{p}^{k/2} + 2q^{k/2}\bar{q}^{k/2} + 2r^{k/2}\bar{r}^{k/2} + 2s^{k/2}\bar{s}^{k/2} \quad (39)$$

$$b_k = A^k + B^k + C^k + D^k + p^k + \bar{p}^k + q^k + \bar{q}^k + r^k + \bar{r}^k + s^k + \bar{s}^k \quad (40)$$

These ligand-inventory functions are introduced into the CI-CFs collected in Table 3. The resulting equations are expanded to give generating functions, where the coefficient of each term $A^a B^b C^c D^d p^p \bar{p}^{\bar{p}} q^q \bar{q}^{\bar{q}} r^r \bar{r}^{\bar{r}} s^s \bar{s}^{\bar{s}}$ ($a+b+c+d+p+\bar{p}+q+\bar{q}+r+\bar{r}+s+\bar{s}=4$) represents the number of quadruplets with the respective composition. Note that a pair of compensated terms, i.e., $\frac{1}{2}(A^a B^b C^c D^d p^p \bar{p}^{\bar{p}} q^q \bar{q}^{\bar{q}} r^r \bar{r}^{\bar{r}} s^s \bar{s}^{\bar{s}} + A^a B^b C^c D^d p^{\bar{p}} \bar{p}^p q^{\bar{q}} \bar{q}^q r^{\bar{r}} \bar{r}^r s^{\bar{s}} \bar{s}^s)$, should be regarded as representing a single quadruplet. Because the terms in the generating functions appear symmetrically, the term $A^a B^b C^c D^d p^p \bar{p}^{\bar{p}} q^q \bar{q}^{\bar{q}} r^r \bar{r}^{\bar{r}} s^s \bar{s}^{\bar{s}}$ can be represented by a partition:

$$[\theta] = [a, b, c, d, p, \bar{p}, q, \bar{q}, r, \bar{r}, s, \bar{s}], \quad (41)$$

where we presume $a \geq b \geq c \geq d$; $p \geq q \geq r \geq s$; $p \geq \bar{p}$, $q \geq \bar{q}$, $r \geq \bar{r}$, and $s \geq \bar{s}$ so as to be adopted as a representative.

Because a generating function has so many complicated terms in general, it is desirable to obtain the coefficient of a specific term selectively. For this purpose, the function `calcCoeffGen` has been developed and stored in the above-mentioned file named

CICFgenCC.func (Appendix A of [43]), which should be loaded beforehand by means of the GAP command `Read`. For example, the coefficients of the terms A^3B (A^3*B) and A^2B^2 (A^2*B^2) appearing in the function $f = (A + B)^4$ are calculated by inputting the following commands:

```
gap> Read("c:/fujita0/fujita2016/TdsI-GAP/calc-GAP/CICFgenCC.gapfunc");
gap> A := Indeterminate(Rationals, "A"); B := Indeterminate(Rationals, "B");
gap> f := (A + B)^4;
A^4+4*A^3*B+6*A^2*B^2+4*A*B^3+B^4
gap> coeff_A3B := calcCoeffGen(f, [A,B], [3,1]);
4
gap> coeff_A2B2 := calcCoeffGen(f, [A,B], [2,2]);
6
```

The source list for calculating the coefficients of the generating functions derived from the CI-CFs collected in Table 3 is stored in a work file named `enum-TdsI.gap`, which is attached as Appendix A. The results are shown in Table 4. The data of the \mathbf{T}_d -column and the $\mathbf{T}_{d\hat{\sigma}\hat{I}}$ of Table 4 are consistent with the data of Table 2 of [44], which have been calculated by an alternative procedure without relying on the present computer-oriented representations.

Note that a fraction $1/2$ of the intersection between the $[\theta]_3$ -row and the $\mathbf{T}_{d\hat{\sigma}\hat{I}}$ -column, for example, corresponds to $1 \times \frac{1}{2}(A^3p + A^3\bar{p})$, which means one quadruplet of *RS*-stereoisomers. Thus, the $[\theta]_3$ -row indicates that the one quadruplet of *RS*-stereoisomers corresponds to one pair of enantiomers (the \mathbf{T}_d -column), to two *RS*-astereogenic promolecules ($2 \times \frac{1}{2}(A^3p + A^3\bar{p})$) at the $\mathbf{T}_{\hat{\sigma}}$ -column, to one pair of holantimers (the $\mathbf{T}_{\hat{I}}$ -column), and to two promolecules ($2 \times \frac{1}{2}(A^3p + A^3\bar{p})$) at the \mathbf{T} -column).

A representative promolecule for each quadruplet of *RS*-stereoisomers, which is listed in the $\mathbf{T}_{d\hat{\sigma}\hat{I}}$ -column of Table 4, is depicted in Figure 3. The representative is accompanied by the corresponding partition ($[\theta]_1 - [\theta]_{30}$) and its aspect index, which designates [type, *RS*-stereoisomeric group; point group, *RS*-permutation group, ligand-reflection group].

4 Type-Itemized Enumeration

4.1 Type-Itemized CI-CFs for a Tetrahedral Skeleton

Type-itemized enumerations of *RS*-stereoisomers have been reported recently [39, 40], where CI-CFs modulated by type-IV or type-V quadruplets have been defined to calculate type-itemized CI-CFs. Modulated CI-CFs by type-V quadruplets (Definition 1 of [40]) are adopted here by relying on the present computer-oriented representations.

A modulated CI-CF of the present purpose is calculated as follows:

Table 4. Enumeration of Tetrahedral Promolecules Under the *RS*-Stereoisomeric Group $\mathbf{T}_{d\bar{\sigma}\hat{\tau}}$ and its Subgroups

partition	numbers of promolecules under respective groups				
	\mathbf{T}_d	$\mathbf{T}_{\bar{\sigma}}$	$\mathbf{T}_{\hat{\tau}}$	\mathbf{T}	$\mathbf{T}_{d\bar{\sigma}\hat{\tau}}$
	$[\theta]_1 = [4, 0, 0, 0, 0, 0, 0, 0, 0, 0, 0]$	1	1	1	1
$[\theta]_2 = [3, 1, 0, 0, 0, 0, 0, 0, 0, 0, 0]$	1	1	1	1	1
$[\theta]_3 = [3, 0, 0, 0, 1, 0, 0, 0, 0, 0, 0]$	1/2	1	1/2	1	1/2
$[\theta]_4 = [2, 2, 0, 0, 0, 0, 0, 0, 0, 0, 0]$	1	1	1	1	1
$[\theta]_5 = [2, 0, 0, 0, 2, 0, 0, 0, 0, 0, 0]$	1/2	1	1/2	1	1/2
$[\theta]_6 = [2, 1, 1, 0, 0, 0, 0, 0, 0, 0, 0]$	1	1	1	1	1
$[\theta]_7 = [2, 1, 0, 0, 1, 0, 0, 0, 0, 0, 0]$	1/2	1	1/2	1	1/2
$[\theta]_8 = [2, 0, 0, 0, 1, 1, 0, 0, 0, 0, 0]$	1	1	1	1	1
$[\theta]_9 = [2, 0, 0, 0, 1, 0, 1, 0, 0, 0, 0]$	1/2	1	1/2	1	1/2
$[\theta]_{10} = [1, 1, 1, 1, 0, 0, 0, 0, 0, 0, 0]$	1	1	2	2	1
$[\theta]_{11} = [1, 1, 1, 0, 1, 0, 0, 0, 0, 0, 0]$	1	1	1	2	1/2
$[\theta]_{12} = [1, 1, 0, 0, 2, 0, 0, 0, 0, 0, 0]$	1/2	1	1/2	1	1/2
$[\theta]_{13} = [1, 1, 0, 0, 1, 1, 0, 0, 0, 0, 0]$	2	1	1	2	1
$[\theta]_{14} = [1, 1, 0, 0, 1, 0, 1, 0, 0, 0, 0]$	1	1	1	2	1/2
$[\theta]_{15} = [1, 0, 0, 0, 3, 0, 0, 0, 0, 0, 0]$	1/2	1	1/2	1	1/2
$[\theta]_{16} = [1, 0, 0, 0, 2, 1, 0, 0, 0, 0, 0]$	1/2	1	1/2	1	1/2
$[\theta]_{17} = [1, 0, 0, 0, 2, 0, 1, 0, 0, 0, 0]$	1/2	1	1/2	1	1/2
$[\theta]_{18} = [1, 0, 0, 0, 1, 1, 1, 0, 0, 0, 0]$	1	1	1	2	1/2
$[\theta]_{19} = [1, 0, 0, 0, 1, 0, 1, 0, 1, 0, 0]$	1	1	1	2	1/2
$[\theta]_{20} = [0, 0, 0, 0, 4, 0, 0, 0, 0, 0, 0]$	1/2	1	1/2	1	1/2
$[\theta]_{21} = [0, 0, 0, 0, 3, 1, 0, 0, 0, 0, 0]$	1/2	1	1/2	1	1/2
$[\theta]_{22} = [0, 0, 0, 0, 3, 0, 1, 0, 0, 0, 0]$	1/2	1	1/2	1	1/2
$[\theta]_{23} = [0, 0, 0, 0, 2, 2, 0, 0, 0, 0, 0]$	1	1	1	1	1
$[\theta]_{24} = [0, 0, 0, 0, 2, 1, 1, 0, 0, 0, 0]$	1/2	1	1/2	1	1/2
$[\theta]_{25} = [0, 0, 0, 0, 2, 0, 2, 0, 0, 0, 0]$	1/2	1	1/2	1	1/2
$[\theta]_{26} = [0, 0, 0, 0, 2, 0, 1, 1, 0, 0, 0]$	1/2	1	1/2	1	1/2
$[\theta]_{27} = [0, 0, 0, 0, 2, 0, 1, 0, 1, 0, 0]$	1/2	1	1/2	1	1/2
$[\theta]_{28} = [0, 0, 0, 0, 1, 1, 1, 1, 0, 0, 0]$	1	1	2	2	1
$[\theta]_{29} = [0, 0, 0, 0, 1, 1, 1, 0, 1, 0, 0]$	1	1	1	2	1/2
$[\theta]_{30} = [0, 0, 0, 0, 1, 0, 1, 0, 1, 0, 1]$	1	1	1	2	1/2

		<i>RS</i> -astereogenic	<i>RS</i> -stereogenic
chiral		Type I [-, -, a] <div style="display: flex; justify-content: space-around; align-items: center;"> <div style="text-align: center;"> <p>5 ($[\theta]_{10}$) [I, C_2; C_1, C_1, C_2]</p> </div> <div style="text-align: center;"> <p>6 ($[\theta]_{28}$) [I, C_2; C_1, C_1, C_2]</p> </div> </div>	
		Type II [-, a, -] <div style="display: flex; justify-content: space-around; align-items: center;"> <div style="text-align: center;"> <p>7 ($[\theta]_{20}$) [II, T_2; T, T_2, T]</p> </div> <div style="text-align: center;"> <p>8 ($[\theta]_{24}$) [II, C_{2v}; C_2, C_{2v}, C_2]</p> </div> <div style="text-align: center;"> <p>9 ($[\theta]_{16}$) [II, C_{3v}; C_3, C_{3v}, C_3]</p> </div> </div> <div style="display: flex; justify-content: space-around; align-items: center; margin-top: 10px;"> <div style="text-align: center;"> <p>10 ($[\theta]_{22}$) [II, C_{3v}; C_3, C_{3v}, C_3]</p> </div> <div style="text-align: center;"> <p>11 ($[\theta]_{21}$) [II, C_{3v}; C_3, C_{3v}, C_3]</p> </div> <div style="text-align: center;"> <p>12 ($[\theta]_8$) [II, C_{2v}; C_2, C_{2v}, C_2]</p> </div> </div> <div style="display: flex; justify-content: space-around; align-items: center; margin-top: 10px;"> <div style="text-align: center;"> <p>13 ($[\theta]_{25}$) [II, C_{2v}; C_2, C_{2v}, C_2]</p> </div> <div style="text-align: center;"> <p>14 ($[\theta]_7$) [III, C_2; C_1, C_2, C_1]</p> </div> <div style="text-align: center;"> <p>15 ($[\theta]_9$) [III, C_2; C_1, C_2, C_1]</p> </div> </div> <div style="display: flex; justify-content: space-around; align-items: center; margin-top: 10px;"> <div style="text-align: center;"> <p>16 ($[\theta]_{12}$) [II, C_2; C_1, C_2, C_1]</p> </div> <div style="text-align: center;"> <p>17 ($[\theta]_{16}$) [III, C_2; C_1, C_2, C_1]</p> </div> <div style="text-align: center;"> <p>18 ($[\theta]_{17}$) [II, C_2; C_1, C_2, C_1]</p> </div> </div> <div style="display: flex; justify-content: space-around; align-items: center; margin-top: 10px;"> <div style="text-align: center;"> <p>19 ($[\theta]_{21}$) [II, C_2; C_1, C_2, C_1]</p> </div> <div style="text-align: center;"> <p>20 ($[\theta]_{26}$) [II, C_2; C_1, C_2, C_1]</p> </div> <div style="text-align: center;"> <p>21 ($[\theta]_{27}$) [III, C_2; C_1, C_2, C_1]</p> </div> </div>	

Figure 3. Reference promolecules of quadruplets of *RS*-stereoisomers (Types I to V) for tetrahedral promolecules. A quadruplet of *RS*-stereoisomers is counted once under the action of the *RS*-stereoisomeric group $T_{d\bar{3}2}$, so that an arbitrary promolecule is depicted as a representative of each quadruplet of *RS*-stereoisomers. The partition (cf. Table 4) and its aspect index (designating [type, *RS*-stereoisomeric group; point group, *RS*-permutation group, ligand-reflection group]) are attached to the compound number of each promolecule.

Table 5. Type-Itemized CI-CFs under the Action of the *RS*-Stereoisomeric Group $\mathbf{T}_{d\bar{\sigma}\hat{f}}$ on a Tetrahedral Skeleton

Type (Type Index)	CI-CF under the <i>RS</i> -Stereoisomeric Group $\mathbf{T}_{d\bar{\sigma}\hat{f}}$
Type I ([-, -, a])	$\text{CICF_I} := -\text{mCICF_Td} + \text{CICF_TI}$ $= 1/24*a_1^4-1/4*a_1^2*a_2+1/3*a_1*a_3+1/8*c_2^2-1/4*c_2*a_2$ $+1/4*a_2^2-1/4*c_4$
Type II ([-, a, -])	$\text{CICF_II} := -\text{mCICF_Td} + \text{CICF_Ts}$ $= 1/4*b_1^2*b_2-1/4*a_1^2*a_2-1/4*c_2*a_2+1/4*a_2^2-1/4*c_4+1/4*b_4$
Type III ([-, -, -])	$\text{CICF_III} := \text{mCICF_Td} - \text{CICF_TdsI}$ $= 1/48*b_1^4-1/48*a_1^4-1/8*b_1^2*b_2-1/8*a_1^2*c_2+1/4*a_1^2*a_2$ $+1/6*b_1*b_3-1/6*a_1*a_3-1/16*c_2^2$ $+1/4*c_2*a_2+1/16*b_2^2-1/4*a_2^2+1/8*c_4-1/8*b_4$
Type IV ([a, a, a])	$\text{CICF_IV} := -\text{CICF_T} + 2*\text{mCICF_Td}$ $= 1/2*a_1^2*a_2+1/2*c_2*a_2-1/2*a_2^2+1/2*c_4$
Type V ([a, -, -])	$\text{CICF_V} := \text{CICF_T} - \text{mCICF_Td} - \text{CICF_Ts} - \text{CICF_TI} + 2*\text{CICF_TdsI}$ $= 1/4*a_1^2*c_2-1/4*a_1^2*a_2-1/4*c_2*a_2+1/4*a_2^2$

```
gap> CICF_Vx := (1/4)*(a_1^2*c_2 - a_1^2*a_2 - a_2*c_2 + a_2^2);
1/4*a_1^2*c_2-1/4*a_1^2*a_2-1/4*c_2*a_2+1/4*a_2^2
gap> mCICF_Td := CICF_Td - CICF_Vx;
1/24*b_1^4+1/4*a_1^2*a_2+1/3*b_1*b_3+1/4*c_2*a_2+1/8*b_2^2-1/4*a_2^2+1/4*c_4
```

The CI-CF denoted by CICF_Vx is a CI-CF for calculating type-V quadruplets under the action of the *RS*-stereoisomeric group $\mathbf{T}_{d\bar{\sigma}\hat{f}}$ on a tetrahedral skeleton (Eq. 64 of [40]). The corresponding modulated CI-CF (mCICF_Td) is calculated by $\text{CICF_Td} - \text{CICF_Vx}$, where the modulated CI-CF (Eq. 65 of [40]) is interpreted to rely on the present computer-oriented representations.

The set of CI-CFs collected in Table 3 (CICF_Ts , CICF_TI , CICF_T , and CICF_TdsI) and the modulated CI-CF (mCICF_Td in place of CICF_Td) are used to calculate type-itemized CI-CFs (denoted as CICF_I to CICF_V) according to Eqs. 7–11 of [40]. The results are summarized in Table 5. They are identical with the CI-CFs reported in [40] (Eqs. 66–70), which have been obtained without relying on the present computer-oriented representations.

4.2 Type-Itemized Enumeration of *RS*-Stereoisomers Derived from a Tetrahedral Skeleton

To accomplish type-itemized enumeration under the *RS*-stereoisomeric group $\mathbf{T}_{d\bar{\sigma}\hat{f}}$, the ligand ligand-inventory functions shown in Eqs. 38–40 are introduced to the type-itemized

CI-CFs (CICF_I to CICF_V) collected in Table 5. The resulting equations are expanded to give generating functions (\mathbf{f}_I to \mathbf{f}_V) in a parallel way to Subsection 3.3. The coefficient of each term in the generating functions is calculated by using the function `calcCoeffGen` described above.

The source list for calculating the coefficients of the generating functions derived from the CI-CFs collected in Table 5 is stored in a work file named `enumType-TdsI1.gap`, which is attached as Appendix B. The results are shown in Table 6. The data of Table 6 are consistent with the generating functions reported in Eqs. 77–81 of [39], which have been calculated by an alternative procedure without relying on the present computer-oriented representations.

Each type-itemized number of Table 6 is concerned with the number of quadruplets of *RS*-stereoisomers which are inequivalent under the *RS*-stereoisomeric group $\mathbf{T}_{d\bar{\sigma}\hat{T}}$. This means that one quadruplet of *RS*-stereoisomers is counted once, so that the value 1/2 at the intersection between the $[\theta]_3$ -row and the type-II column, for example, corresponds to $1 \times \frac{1}{2}(A^3P + A^3\bar{P})$.

Table 6 indicates the presence of two type-I quadruplets of *RS*-stereoisomers, of fifteen type-II quadruplets (due to 15/2), of six type-III quadruplets (due to 6/2), of six type-IV quadruplets, and of one type-V quadruplet. The representative promolecules of these quadruplets are depicted in Figure 3, where they are itemized into type I to type V.

5 Conclusion

Computer-oriented representations of *RS*-stereoisomeric groups have been developed, where (roto)reflections (or ligand-reflections) and rotations (or *RS*-permutations) are differentiated by means of a mirror-coset representation. Thereby, two subgroups isomorphic under an *RS*-stereoisomeric group, i.e., a point group and an *RS*-permutation group, are differentiated so as to specify chirality and *RS*-stereogenicity as two kinds of handedness. The processes of combinatorial enumeration under an *RS*-stereoisomeric group, i.e.,

1. the construction of the *RS*-stereoisomeric group,
2. the calculation of the corresponding CI-CF,
3. the calculation of the corresponding generating function, and
4. the evaluation of the coefficient of each term appearing in the generating function

Table 6. Type-Itemized Enumeration of *RS*-Stereoisomers Under $\mathbf{T}_{d\hat{\sigma}\hat{\tau}}$

	partition	type-itemized numbers				
		I	II	III	IV	V
$[\theta]_1 =$	[4, 0, 0, 0, 0, 0, 0, 0, 0, 0, 0]	0	0	0	1	0
$[\theta]_2 =$	[3, 1, 0, 0, 0, 0, 0, 0, 0, 0, 0]	0	0	0	1	0
$[\theta]_3 =$	[3, 0, 0, 0, 1, 0, 0, 0, 0, 0, 0]	0	1/2	0	0	0
$[\theta]_4 =$	[2, 2, 0, 0, 0, 0, 0, 0, 0, 0, 0]	0	0	0	1	0
$[\theta]_5 =$	[2, 0, 0, 0, 2, 0, 0, 0, 0, 0, 0]	0	1/2	0	0	0
$[\theta]_6 =$	[2, 1, 1, 0, 0, 0, 0, 0, 0, 0, 0]	0	0	0	1	0
$[\theta]_7 =$	[2, 1, 0, 0, 1, 0, 0, 0, 0, 0, 0]	0	1/2	0	0	0
$[\theta]_8 =$	[2, 0, 0, 0, 1, 1, 0, 0, 0, 0, 0]	0	0	0	1	0
$[\theta]_9 =$	[2, 0, 0, 0, 1, 0, 1, 0, 0, 0, 0]	0	1/2	0	0	0
$[\theta]_{10} =$	[1, 1, 1, 1, 0, 0, 0, 0, 0, 0, 0]	1	0	0	0	0
$[\theta]_{11} =$	[1, 1, 1, 0, 1, 0, 0, 0, 0, 0, 0]	0	0	1/2	0	0
$[\theta]_{12} =$	[1, 1, 0, 0, 2, 0, 0, 0, 0, 0, 0]	0	1/2	0	0	0
$[\theta]_{13} =$	[1, 1, 0, 0, 1, 1, 0, 0, 0, 0, 0]	0	0	0	0	1
$[\theta]_{14} =$	[1, 1, 0, 0, 1, 0, 1, 0, 0, 0, 0]	0	0	1/2	0	0
$[\theta]_{15} =$	[1, 0, 0, 0, 3, 0, 0, 0, 0, 0, 0]	0	1/2	0	0	0
$[\theta]_{16} =$	[1, 0, 0, 0, 2, 1, 0, 0, 0, 0, 0]	0	1/2	0	0	0
$[\theta]_{17} =$	[1, 0, 0, 0, 2, 0, 1, 0, 0, 0, 0]	0	1/2	0	0	0
$[\theta]_{18} =$	[1, 0, 0, 0, 1, 1, 1, 0, 0, 0, 0]	0	0	1/2	0	0
$[\theta]_{19} =$	[1, 0, 0, 0, 1, 0, 1, 0, 1, 0, 0]	0	0	1/2	0	0
$[\theta]_{20} =$	[0, 0, 0, 0, 4, 0, 0, 0, 0, 0, 0]	0	1/2	0	0	0
$[\theta]_{21} =$	[0, 0, 0, 0, 3, 1, 0, 0, 0, 0, 0]	0	1/2	0	0	0
$[\theta]_{22} =$	[0, 0, 0, 0, 3, 0, 1, 0, 0, 0, 0]	0	1/2	0	0	0
$[\theta]_{23} =$	[0, 0, 0, 0, 2, 2, 0, 0, 0, 0, 0]	0	0	0	1	0
$[\theta]_{24} =$	[0, 0, 0, 0, 2, 1, 1, 0, 0, 0, 0]	0	1/2	0	0	0
$[\theta]_{25} =$	[0, 0, 0, 0, 2, 0, 2, 0, 0, 0, 0]	0	1/2	0	0	0
$[\theta]_{26} =$	[0, 0, 0, 0, 2, 0, 1, 1, 0, 0, 0]	0	1/2	0	0	0
$[\theta]_{27} =$	[0, 0, 0, 0, 2, 0, 1, 0, 1, 0, 0]	0	1/2	0	0	0
$[\theta]_{28} =$	[0, 0, 0, 0, 1, 1, 1, 1, 0, 0, 0]	1	0	0	0	0
$[\theta]_{29} =$	[0, 0, 0, 0, 1, 1, 1, 0, 1, 0, 0]	0	0	1/2	0	0
$[\theta]_{30} =$	[0, 0, 0, 0, 1, 0, 1, 0, 1, 0, 1]	0	0	1/2	0	0
	total	2	15/2	6/2	6	1

are computerized by using the GAP system.

Appendix A. Source List of `enum-TdsI.gap` for Enumerating Tetrahedral *RS*-Stereoisomers

The following program for combinatorial enumeration of *RS*-stereoisomers based on a tetrahedral skeleton is stored in a file named `enum-TdsI.gap` (an arbitrary name), which is placed in a work directory named `c:/fujita0/fujita2016/TdsI-GAP/calcul-GAP/` (an arbitrary name). To use the functions `CalcConjClassCICF` and `calcCoeffGen`, the file `CICFgenCC.gapfunc` is beforehand loaded. To execute this file, the first line commented out by the `#` symbol is copied and paste after the `gap>` prompt in the command prompt of the Windows operating system. The output is stored in the log file named `enum-TdsIlog.txt` (an arbitrary name), which contains the data for constructing Table 4. Each pair of lowercase letters p/\bar{p} , q/\bar{q} , r/\bar{r} , or s/\bar{s} in the ligand-inventory functions (Eqs. 39 and e40) is replaced by a pair of an lowercase letter and the corresponding uppercase letter (e.g., p/P).

```
#Read("c:/fujita0/fujita2016/TdsI-GAP/calcul-GAP/enum-TdsI.gap");
LogTo("c:/fujita0/fujita2016/TdsI-GAP/calcul-GAP/enum-TdsIlog.txt");

Read("c:/fujita0/fujita2016/TdsI-GAP/calcul-GAP/CICFgenCC.gapfunc"); #Loading of CICFgenCC.gapfunc

gen_Td := [(1,3)(2,4), (2,3,4), (1,3)(5,6)]; Td := Group(gen_Td);
CICF_Td := CalcConjClassCICF(Td, 4, 6);

gen_Ts := [(1,3)(2,4), (2,3,4), (1,3)]; Ts := Group(gen_Ts);
CICF_Ts := CalcConjClassCICF(Ts, 4, 6);

gen_TI := [(1,3)(2,4), (2,3,4), (5,6)]; TI := Group(gen_TI);
CICF_TI := CalcConjClassCICF(TI, 4, 6);

gen_T := [(1,3)(2,4), (2,3,4)]; T := Group(gen_T);
CICF_T := CalcConjClassCICF(T, 4, 6);

gen_1 := [(1,3)(2,4), (2,3,4), (1,3)(5,6), (5,6)]; TdsI := Group(gen_1);
CICF_TdsI := CalcConjClassCICF(TdsI, 4, 6);

A := Indeterminate(Rationals, "A"); B := Indeterminate(Rationals, "B");
C := Indeterminate(Rationals, "C"); D := Indeterminate(Rationals, "D");
p := Indeterminate(Rationals, "p"); P := Indeterminate(Rationals, "P");
q := Indeterminate(Rationals, "q"); Q := Indeterminate(Rationals, "Q");
r := Indeterminate(Rationals, "r"); R := Indeterminate(Rationals, "R");
s := Indeterminate(Rationals, "s"); S := Indeterminate(Rationals, "S");

b_1 := Indeterminate(Rationals, "b_1"); b_2 := Indeterminate(Rationals, "b_2");
b_3 := Indeterminate(Rationals, "b_3"); b_4 := Indeterminate(Rationals, "b_4");
a_1 := Indeterminate(Rationals, "a_1"); a_2 := Indeterminate(Rationals, "a_2");
a_3 := Indeterminate(Rationals, "a_3"); a_4 := Indeterminate(Rationals, "a_4");
c_2 := Indeterminate(Rationals, "c_2"); c_4 := Indeterminate(Rationals, "c_4");

aa_1 := A + B + C + D; aa_2 := A^2 + B^2 + C^2 + D^2;
aa_3 := A^3 + B^3 + C^3 + D^3; aa_4 := A^4 + B^4 + C^4 + D^4;
bb_1 := A + B + C + D + p + q + r + s + P + Q + R + S;
bb_2 := A^2 + B^2 + C^2 + D^2 + p^2 + q^2 + r^2 + s^2 + P^2 + Q^2 + R^2 + S^2;
bb_3 := A^3 + B^3 + C^3 + D^3 + p^3 + q^3 + r^3 + s^3 + P^3 + Q^3 + R^3 + S^3;
bb_4 := A^4 + B^4 + C^4 + D^4 + p^4 + q^4 + r^4 + s^4 + P^4 + Q^4 + R^4 + S^4;
cc_2 := A^2 + B^2 + C^2 + D^2 + 2*p*p + 2*q*q + 2*r*r + 2*s*s;
```

```

cc_4 := A^4 + B^4 + C^4 + D^4 + 2*p^2*P^2 + 2*q^2*Q^2 + 2*r^2*R^2 + 2*s^2*S^2;

f_Td := Value(CICF_Td, [a_1, a_2, a_3, a_4, b_1, b_2, b_3, b_4, c_2, c_4],
[aa_1, aa_2, aa_3, aa_4, bb_1, bb_2, bb_3, bb_4, cc_2, cc_4]);

f_Ts := Value(CICF_Ts, [a_1, a_2, a_3, a_4, b_1, b_2, b_3, b_4, c_2, c_4],
[aa_1, aa_2, aa_3, aa_4, bb_1, bb_2, bb_3, bb_4, cc_2, cc_4]);

f_TI := Value(CICF_TI, [a_1, a_2, a_3, a_4, b_1, b_2, b_3, b_4, c_2, c_4],
[aa_1, aa_2, aa_3, aa_4, bb_1, bb_2, bb_3, bb_4, cc_2, cc_4]);

f_T := Value(CICF_T, [a_1, a_2, a_3, a_4, b_1, b_2, b_3, b_4, c_2, c_4],
[aa_1, aa_2, aa_3, aa_4, bb_1, bb_2, bb_3, bb_4, cc_2, cc_4]);

f_TdsI := Value(CICF_TdsI, [a_1, a_2, a_3, a_4, b_1, b_2, b_3, b_4, c_2, c_4],
[aa_1, aa_2, aa_3, aa_4, bb_1, bb_2, bb_3, bb_4, cc_2, cc_4]);

list_partitions := [];
calcCoeffGenTdsI := function(list_partitions)
local list_ligand_L, l_pp;
list_ligand_L := [A,B,C,D,p,P,q,Q,r,R,s,S];
l_pp := list_partitions;
Print("$", l_pp, "$&&");
calcCoeffGen(f_Td, list_ligand_L, list_partitions), "_&&";
calcCoeffGen(f_Ts, list_ligand_L, list_partitions), "_&&";
calcCoeffGen(f_TI, list_ligand_L, list_partitions), "_&&";
calcCoeffGen(f_T, list_ligand_L, list_partitions), "_&&";
calcCoeffGen(f_TdsI, list_ligand_L, list_partitions), "_&&\\n");
end;

#"Print A4";
calcCoeffGenTdsI([4,0,0,0,0,0,0,0,0,0]);
#"Print A3";
calcCoeffGenTdsI([3,1,0,0,0,0,0,0,0,0]); calcCoeffGenTdsI([3,0,0,0,1,0,0,0,0,0]);
#"Print A2";
calcCoeffGenTdsI([2,2,0,0,0,0,0,0,0,0]); calcCoeffGenTdsI([2,0,0,0,2,0,0,0,0,0]);
calcCoeffGenTdsI([2,1,1,0,0,0,0,0,0,0]); calcCoeffGenTdsI([2,1,0,0,1,0,0,0,0,0]);
calcCoeffGenTdsI([2,0,0,0,1,1,0,0,0,0]); calcCoeffGenTdsI([2,0,0,0,1,0,1,0,0,0]);
#"Print A1";
calcCoeffGenTdsI([1,1,1,1,0,0,0,0,0,0]); calcCoeffGenTdsI([1,1,1,0,1,0,0,0,0,0]);
calcCoeffGenTdsI([1,1,0,0,2,0,0,0,0,0]); calcCoeffGenTdsI([1,1,0,0,1,1,0,0,0,0]);
calcCoeffGenTdsI([1,1,0,0,1,0,1,0,0,0,0]); calcCoeffGenTdsI([1,0,0,0,3,0,0,0,0,0]);
calcCoeffGenTdsI([1,0,0,0,2,1,0,0,0,0]); calcCoeffGenTdsI([1,0,0,0,2,0,1,0,0,0,0]);
calcCoeffGenTdsI([1,0,0,0,1,1,1,0,0,0,0]); calcCoeffGenTdsI([1,0,0,0,1,0,1,0,0,0]);
#"Print A0";
calcCoeffGenTdsI([0,0,0,0,4,0,0,0,0,0]); calcCoeffGenTdsI([0,0,0,0,3,1,0,0,0,0]);
calcCoeffGenTdsI([0,0,0,0,3,0,1,0,0,0,0]); calcCoeffGenTdsI([0,0,0,0,2,2,0,0,0,0]);
calcCoeffGenTdsI([0,0,0,0,2,1,1,0,0,0,0]); calcCoeffGenTdsI([0,0,0,0,2,0,2,0,0,0]);
calcCoeffGenTdsI([0,0,0,0,2,0,1,1,0,0,0,0]); calcCoeffGenTdsI([0,0,0,0,2,0,1,0,1,0,0]);
calcCoeffGenTdsI([0,0,0,0,1,1,1,1,0,0,0,0]); calcCoeffGenTdsI([0,0,0,0,1,1,1,0,1,0,0]);
calcCoeffGenTdsI([0,0,0,0,1,0,1,0,1,0,1,0]);

```

```
LogTo();
```

Appendix B. Source List of enumType-TdsI1.gap for Type-Itemized Enumeration of Tetrahedral *RS*-Stereoisomers

The following program for combinatorial enumeration of *RS*-stereoisomers based on a tetrahedral skeleton is stored in a file named `enumType-TdsI1.gap` (an arbitrary name), which is placed in a work directory named `c:/fujita0/fujita2016/TdsI-GAP/calc-GAP/` (an arbitrary name). To use the functions `CalcConjClassCICF` and `calcCoeffGen`, the file `CICFgenCC.gapfunc` is beforehand loaded. To execute this file, the first line commented out by the `#` symbol is copied and paste after the `gap>` prompt in the command

prompt of the Windows operating system. The output is stored in the log file named `enumType-TdsI1log` (an arbitrary name), which contains the data for constructing Table 6. Each pair of lowercase letters p/\bar{p} , q/\bar{q} , r/\bar{r} , or s/\bar{s} in the ligand-inventory functions (Eqs. 39 and e40) is replaced by a pair of an lowercase letter and the corresponding uppercase letter (e.g., p/P).

```
#Read("c:/fujita0/fujita2016/TdsI-GAP/Calc-GAP/enumType-TdsI1.gap");
LogTo("c:/fujita0/fujita2016/TdsI-GAP/Calc-GAP/enumType-TdsI1log.txt");

Read("c:/fujita0/fujita2016/TdsI-GAP/Calc-GAP/CICFgenCC.gapfunc"); #Loading of CICFgenCC.gapfunc

gen_Td := [(1,3)(2,4), (2,3,4), (1,3)(5,6)]; Td := Group(gen_Td);
CICF_Td := CalcConjClassCICF(Td, 4, 6);

gen_Ts := [(1,3)(2,4), (2,3,4), (1,3)]; Ts := Group(gen_Ts);
CICF_Ts := CalcConjClassCICF(Ts, 4, 6);

gen_TI := [(1,3)(2,4), (2,3,4), (5,6)]; TI := Group(gen_TI);
CICF_TI := CalcConjClassCICF(TI, 4, 6);

gen_T := [(1,3)(2,4), (2,3,4)]; T := Group(gen_T);
CICF_T := CalcConjClassCICF(T, 4, 6);

gen_1 := [(1,3)(2,4), (2,3,4), (1,3)(5,6), (5,6)]; TdsI := Group(gen_1);
CICF_TdsI := CalcConjClassCICF(TdsI, 4, 6);

b_1 := Indeterminate(Rationals, "b_1"); b_2 := Indeterminate(Rationals, "b_2");
b_3 := Indeterminate(Rationals, "b_3"); b_4 := Indeterminate(Rationals, "b_4");
a_1 := Indeterminate(Rationals, "a_1"); a_2 := Indeterminate(Rationals, "a_2");
a_3 := Indeterminate(Rationals, "a_3"); a_4 := Indeterminate(Rationals, "a_4");
c_2 := Indeterminate(Rationals, "c_2"); c_4 := Indeterminate(Rationals, "c_4");

#Modulated CICF
CICF_Vx := (1/4)*(a_1^2*c_2 - a_1^2*a_2 - a_2*c_2 + a_2^2);
mCICF_Td := CICF_Td - CICF_Vx;

#Type-Itemized CI-CFs
CICF_I := -mCICF_Td + CICF_TI;
CICF_II := -mCICF_Td + CICF_Ts;
CICF_III := mCICF_Td - CICF_TdsI;
CICF_IV := -CICF_T + 2*mCICF_Td;
CICF_V := CICF_T - mCICF_Td - CICF_Ts - CICF_TI + 2*CICF_TdsI;

#Indeterminates for Enumeration
A := Indeterminate(Rationals, "A"); B := Indeterminate(Rationals, "B");
C := Indeterminate(Rationals, "C"); D := Indeterminate(Rationals, "D");
p := Indeterminate(Rationals, "p"); P := Indeterminate(Rationals, "P");
q := Indeterminate(Rationals, "q"); Q := Indeterminate(Rationals, "Q");
r := Indeterminate(Rationals, "r"); R := Indeterminate(Rationals, "R");
s := Indeterminate(Rationals, "s"); S := Indeterminate(Rationals, "S");

#Ligand-Inventory Functions
aa_1 := A + B + C + D; aa_2 := A^2 + B^2 + C^2 + D^2;
aa_3 := A^3 + B^3 + C^3 + D^3; aa_4 := A^4 + B^4 + C^4 + D^4;
bb_1 := A + B + C + D + p + q + r + s + P + Q + R + S;
bb_2 := A^2 + B^2 + C^2 + D^2 + p^2 + q^2 + r^2 + s^2 + P^2 + Q^2 + R^2 + S^2;
bb_3 := A^3 + B^3 + C^3 + D^3 + p^3 + q^3 + r^3 + s^3 + P^3 + Q^3 + R^3 + S^3;
bb_4 := A^4 + B^4 + C^4 + D^4 + p^4 + q^4 + r^4 + s^4 + P^4 + Q^4 + R^4 + S^4;
cc_2 := A^2 + B^2 + C^2 + D^2 + 2*p*P + 2*q*Q + 2*r*R + 2*s*S;
cc_4 := A^4 + B^4 + C^4 + D^4 + 2*p^2*P^2 + 2*q^2*Q^2 + 2*r^2*R^2 + 2*s^2*S^2;

#Generating Function for Type I to type V
f_I := Value(CICF_I, [a_1, a_2, a_3, a_4, b_1, b_2, b_3, b_4, c_2, c_4],
[aa_1, aa_2, aa_3, aa_4, bb_1, bb_2, bb_3, bb_4, cc_2, cc_4]);

f_II := Value(CICF_II, [a_1, a_2, a_3, a_4, b_1, b_2, b_3, b_4, c_2, c_4],
[aa_1, aa_2, aa_3, aa_4, bb_1, bb_2, bb_3, bb_4, cc_2, cc_4]);
```

```

f_III := Value(CICF_III, [a_1, a_2, a_3, a_4, b_1, b_2, b_3, b_4, c_2, c_4],
[aa_1, aa_2, aa_3, aa_4, bb_1, bb_2, bb_3, bb_4, cc_2, cc_4]);

f_IV := Value(CICF_IV, [a_1, a_2, a_3, a_4, b_1, b_2, b_3, b_4, c_2, c_4],
[aa_1, aa_2, aa_3, aa_4, bb_1, bb_2, bb_3, bb_4, cc_2, cc_4]);

f_V := Value(CICF_V, [a_1, a_2, a_3, a_4, b_1, b_2, b_3, b_4, c_2, c_4],
[aa_1, aa_2, aa_3, aa_4, bb_1, bb_2, bb_3, bb_4, cc_2, cc_4]);

#Function for Constructing Tabular Format
list_partitions := [];
calcCoeffGenType := function(list_partitions)
local list_ligand_L, l_pp;
list_ligand_L := [A,B,C,D,p,P,q,Q,r,R,s,S];
l_pp := list_partitions;
Print("$", l_pp, "$\&\_");
calcCoeffGen(f_I, list_ligand_L, list_partitions), "\&\_";
calcCoeffGen(f_II, list_ligand_L, list_partitions), "\&\_";
calcCoeffGen(f_III, list_ligand_L, list_partitions), "\&\_";
calcCoeffGen(f_IV, list_ligand_L, list_partitions), "\&\_";
calcCoeffGen(f_V, list_ligand_L, list_partitions), "\\\&\_m";
end;

#Print A4";
calcCoeffGenType([4,0,0,0,0,0,0,0,0,0]);
#Print A3";
calcCoeffGenType([3,1,0,0,0,0,0,0,0,0]); calcCoeffGenType([3,0,0,0,1,0,0,0,0,0]);
#Print A2";
calcCoeffGenType([2,2,0,0,0,0,0,0,0,0]); calcCoeffGenType([2,0,0,0,2,0,0,0,0,0]);
calcCoeffGenType([2,1,1,0,0,0,0,0,0,0]); calcCoeffGenType([2,1,0,0,1,0,0,0,0,0]);
calcCoeffGenType([2,0,0,0,1,1,0,0,0,0]); calcCoeffGenType([2,0,0,0,1,0,1,0,0,0]);
#Print A1";
calcCoeffGenType([1,1,1,1,0,0,0,0,0,0]); calcCoeffGenType([1,1,1,0,1,0,0,0,0,0]);
calcCoeffGenType([1,1,0,0,2,0,0,0,0,0]); calcCoeffGenType([1,1,0,0,1,1,0,0,0,0]);
calcCoeffGenType([1,1,0,0,1,0,1,0,0,0,0]); calcCoeffGenType([1,0,0,0,3,0,0,0,0,0]);
calcCoeffGenType([1,0,0,0,2,1,0,0,0,0,0]); calcCoeffGenType([1,0,0,0,2,0,1,0,0,0,0]);
calcCoeffGenType([1,0,0,0,1,1,1,0,0,0,0]); calcCoeffGenType([1,0,0,0,1,0,1,0,0,0]);
#Print A0";
calcCoeffGenType([0,0,0,0,4,0,0,0,0,0]); calcCoeffGenType([0,0,0,0,3,1,0,0,0,0]);
calcCoeffGenType([0,0,0,0,3,0,1,0,0,0,0]); calcCoeffGenType([0,0,0,0,2,2,0,0,0,0]);
calcCoeffGenType([0,0,0,0,2,1,1,0,0,0,0]); calcCoeffGenType([0,0,0,0,2,0,2,0,0,0]);
calcCoeffGenType([0,0,0,0,2,0,1,1,0,0,0]); calcCoeffGenType([0,0,0,0,2,0,1,0,1,0,0]);
calcCoeffGenType([0,0,0,0,1,1,1,1,0,0,0]); calcCoeffGenType([0,0,0,0,1,1,1,0,1,0,0]);
calcCoeffGenType([0,0,0,0,1,0,1,0,1,0,1]);

```

```
LogTo();
```

References

- [1] J. H. van't Hoff, Voorstel tot uitbreiding der tegenwoordig in de scheikunde gebruikte structure-formules in de ruimte; Benevens een daarmee samenhangende opmerking omtrent het verband tusschen optisch vermogen en chemische constitutie van organische verbindingen, *Archives Néerlandaises des Sciences Exactes et Naturelles* **9** (1874) 445–454.
- [2] J. H. van't Hoff, A suggestion looking to the extension into space of the structural formulas at present used in chemistry. And a note upon the relation between the optical activity and the chemical constitution of organic compounds, in: G. M. Richardson (Ed.), *Foundations of Stereochemistry, Memoirs of Pasteur, van't Hoff, Le Bel, and Wislicenus*, New York, 1901, pp. 35–46.

- [3] J. A. Le Bel, Sur les relations qui existent entre les formules atomiques des corps organique et le pouvoir rotatoire de leurs dissolutions, *Bull. Soc. Chim. Fr. (2)* **22** (1874) 337–347.
- [4] J. A. Le Bel, On the relations which exist between the atomic formulas of organic compounds and the rotatory power of their solutions, in: G. M. Richardson (Ed.), *Foundations of Stereochemistry, Memoirs of Pasteur, van't Hoff, Le Bel, and Wislicenus*, New York, 1901, pp. 47–60.
- [5] G. E. McCasland, *A New General System for the Naming of Stereoisomers*, Chem. Abstracts, Columbus, 1953.
- [6] L. Pasteur, Recherches sur la dissymetrie moléculaire des produits organiques naturels, in: P. Vallery-Radot (Ed.), *Œuvre de Pasteur*, Masson et C^{ie}, Paris, 1922, pp. 314–344.
- [7] W. Thomson (Lord Kelvin), *The Molecular Tactics of a Crystal*, Clarendon, Oxford, 1894.
- [8] E. Fischer, Über die Configuration des Traubenzuckers und seine Isomeren. I, *Ber. Dtsch. chem. Ges.* **24** (1891) 1836–1845.
- [9] E. Fischer, Über die Configuration des Traubenzuckers und seine Isomeren. II, *Ber. Dtsch. chem. Ges.* **24** (1891) 2683–2687.
- [10] V. Prelog, G. Helmchen, Pseudoasymmetrie in der organischen Chemie, *Helv. Chim. Acta* **55** (1972) 2581–2598.
- [11] V. Prelog, G. Helmchen, Basic principles of the CIP-system and proposal for a revision, *Angew. Chem. Int. Ed. Eng.* **21** (1982) 567–583.
- [12] G. Helmchen, A. General Aspects. 1. Nomenclature and vocabulary of organic stereochemistry, in: G. Helmchen, R. W. Hoffmann, J. Mulzer, E. Schaumann (Eds.), *Stereoselective Synthesis. Methods of Organic Chemistry (Houben-Weyl). Workbench Edition E21*, Georg Thieme, Stuttgart, 1996, pp. 1–74.
- [13] E. L. Eliel, Infelicitous stereochemical nomenclature, *Chirality* **9** (1997) 428–430.
- [14] G. Helmchen, Glossary of problematic terms in organic stereochemistry, *Enantiomer* **2** (1997) 315–318.
- [15] K. Mislow, Stereochemical terminology and its discontents, *Chirality* **14** (2002) 126–134.

- [16] J. Gal, Stereochemical vocabulary for structures that are chiral but not asymmetric: History, analysis, and proposal for a rational terminology, *Chirality* **23** (2011) 647–659.
- [17] K. Mislow, J. Siegel, Stereoisomerism and local chirality, *J. Am. Chem. Soc.* **106** (1984) 3319–3328.
- [18] S. Fujita, The stereoisogram approach for remedying discontents of stereochemical terminology, *Tetrahedron: Asymmetry* **25** (2014) 1612–1623.
- [19] S. Fujita, Stereogenicity revisited. Proposal of holantimers for comprehending the relationship between stereogenicity and chirality, *J. Org. Chem.* **69** (2004) 3158–3165.
- [20] S. Fujita, Pseudoasymmetry, stereogenicity, and the *RS*-nomenclature comprehended by the concepts of holantimers and stereoisograms, *Tetrahedron* **60** (2004) 11629–11638.
- [21] S. Fujita, *Mathematical Stereochemistry*, De Gruyter, Berlin, 2015.
- [22] S. Fujita, Three aspects of an absolute configuration on the basis of the stereoisogram approach and revised terminology on related stereochemical concepts, *J. Math. Chem.* **52** (2014) 1514–1534.
- [23] S. Fujita, Stereoisograms for reorganizing the theoretical foundations of stereochemistry and stereoisomerism: I. Diagrammatic representations of *RS*-stereoisomeric groups for integrating point groups and *RS*-permutation groups, *Tetrahedron: Asymmetry* **25** (2014) 1153–1168.
- [24] S. Fujita, Stereoisograms for reorganizing the theoretical foundations of stereochemistry and stereoisomerism: II. Rational avoidance of misleading standpoints for *R/S*-stereodescriptors of the Cahn–Ingold–Prelog system, *Tetrahedron: Asymmetry* **25** (2014) 1169–1189.
- [25] S. Fujita, Stereoisograms for reorganizing the theoretical foundations of stereochemistry and stereoisomerism: III. Rational avoidance of misleading standpoints for *Pro-R/Pro-S*-descriptors, *Tetrahedron: Asymmetry* **25** (2014) 1190–1204.
- [26] S. Fujita, Chirality fittingness of an orbit governed by a coset representation. Integration of point-group and permutation-group theories to treat local chirality and prochirality, *J. Am. Chem. Soc.* **112** (1990) 3390–3397.
- [27] S. Fujita, *Symmetry and Combinatorial Enumeration in Chemistry*, Springer–Verlag, Berlin, 1991.

- [28] S. Fujita, *Diagrammatical Approach to Molecular Symmetry and Enumeration of Stereoisomers*, Univ. Kragujevac, Kragujevac, 2007.
- [29] S. Fujita, Symmetry-itemized enumeration of quadruplets of *RS*-stereoisomers: I — The fixed-point matrix method of the USCI approach combined with the stereoisogram approach, *J. Math. Chem.* **52** (2014) 508–542.
- [30] S. Fujita, Symmetry-itemized enumeration of quadruplets of *RS*-stereoisomers: II — The partial-cycle-index method of the USCI approach combined with the stereoisogram approach, *J. Math. Chem.* **52** (2014) 543–574.
- [31] S. Fujita, Symmetry-itemized enumeration of *RS*-stereoisomers of allenes. I. The fixed-point matrix method of the USCI approach combined with the stereoisogram approach, *J. Math. Chem.* **52** (2014) 1717–1750.
- [32] S. Fujita, Symmetry-itemized enumeration of *RS*-stereoisomers of allenes. II. The partial-cycle-index method of the USCI approach combined with the stereoisogram approach, *J. Math. Chem.* **52** (2014) 1751–1793.
- [33] S. Fujita, Stereoisograms for three-membered heterocycles: I. Symmetry-itemized enumeration of oxiranes under an *RS*-stereoisomeric group, *J. Math. Chem.* **53** (2015) 260–304.
- [34] S. Fujita, Itemized enumeration of quadruplets of *RS*-stereoisomers under the action of *RS*-stereoisomeric groups, *MATCH Commun. Math. Comput. Chem.* **61** (2009) 71–115.
- [35] S. Fujita, Graphs to chemical structures 1. Sphericity indices of cycles for stereochemical extension of Pólya's theorem, *Theor. Chem. Acc.* **113** (2005) 73–79.
- [36] S. Fujita, Graphs to chemical structures 2. Extended sphericity indices of cycles for stereochemical extension of Pólya's coronas, *Theor. Chem. Acc.* **113** (2005) 80–86.
- [37] S. Fujita, Graphs to chemical structures 3. General theorems with the use of different sets of sphericity indices for combinatorial enumeration of nonrigid stereoisomers, *Theor. Chem. Acc.* **115** (2006) 37–53.
- [38] S. Fujita, *Combinatorial Enumeration of Graphs, Three-Dimensional Structures, and Chemical Compounds*, Univ. Kragujevac, Kragujevac, 2013.
- [39] S. Fujita, Type-itemized enumeration of quadruplets of *RS*-stereoisomers. I. Cycle indices with chirality fittingness modulated by type-IV quadruplets, *J. Math. Chem.* **54** (2016) 286–309.

- [40] S. Fujita, Type-itemized enumeration of quadruplets of *RS*-stereoisomers: II. Cycle indices with chirality fittingness modulated by type-V quadruplets, *J. Math. Chem.* **54** (2016) 310–330.
- [41] S. Fujita, Type-itemized enumeration of *RS*-stereoisomers of octahedral complexes, *Iranian J. Math. Chem.* **7** (2016) 113–153.
- [42] S. Fujita, Computer-oriented representations of point groups and cycle indices with chirality fittingness (CI-CFs) calculated by the GAP system. Enumeration of three-dimensional structures of ligancy 4 by Fujita’s proligand method, *MATCH Commun. Math. Comput. Chem.* **76** (2016) 379–400.
- [43] S. Fujita, Computer-oriented representations of O_n -skeletons for supporting combinatorial enumeration by Fujita’s proligand method. GAP calculation of cycle indices with chirality fittingness (CI-CFs), *MATCH Commun. Math. Comput. Chem.* **77** (2017) in press.
- [44] S. Fujita, Combinatorial approach to group hierarchy for stereoskeletons of ligancy 4, *J. Math. Chem.* **53** (2015) 1010–1053.